UNIVERSITÀ
DEGLI STUDI
DI PADOVA

Dipartimento di Pediatria

SCUOLA DI DOTTORATO DI RICERCA IN MEDICINA DELLO SVILUPPO E SCIENZE DELLA PROGRAMMAZIONE
INDIRIZZO SCIENZE CHIRURGICHE PEDIATRICHE E SPERIMENTALI
XXIV CICLO

Differentiation potential and metabolic analysis of satellite cells and amniotic fluid stem cells

Direttore della Scuola e coordinatore di indirizzo:
Ch.mo Prof. Giuseppe Basso

Supervisore:
Ch.mo Prof. Piergiorgio Gamba

Dottorando: Andrea Repele

"La scienza può solo accertare ciò che è, ma non ciò che dovrebbe essere, ed al di fuori del suo ambito restano necessari i giudizi di valori di ogni genere."

Albert Einstein, Pensieri degli anni difficili

Table of Contents

Abstract

We have recently characterized two distinct populations of Satellite Cells (SCs), defined as Low Proliferative Clones (LPC) and High Proliferative Clones (HPC), that differ for proliferation, regenerative potential and mitochondrial coupling efficiency. In here, we have deep investigated their cell biology and characterized features that remark their intrinsic differences retrievable also at the initial phases of their cloning. LPC and HPC can indeed be distinguished for characteristic mitochondrial membrane potential ($\Delta\Psi_m$) just after isolation from their parental fibre. This is merged by mitochondrial redox state -measured via NAD^+/NADH analysis- and alternative respiratory CO_2 production in cloned cells, which are accountable for metabolic differences reflected by alternative expression of the glycolytic enzyme Pfkfb3. In addition also mitochondrial Ca^{2+} handling and the sensitivity to apoptosis triggered via the intrinsic pathway are modified as well as the size of the mitochondrial network. In conclusion, we were able to determine which clone represents the suitable stem cell within the SCs population. These further experimental observations report novel physiological features in the cell biology of SCs populations before and after cloning, highlighting an intrinsic heterogeneity on which the stemness of the satellite cell is likely to depend.

In the second part of my work we have also investigated their potential to trans-differentiate into smooth muscle cells. Enteric Nervous System normally interacts with muscle cells to control the peristaltic and secretory activity of the gut wall. Incomplete gut colonization by neural crest cells causes Hirschsprung's disease, characterized by aganglionosis of the distal bowel. Multipotent, self-renewing enteric precursor neurosphere-like bodies (NLBs) -capable of generating neurons and glia derived from the neural crest- can be isolated from the gut of mice, rats, and human and they are able to colonize the gut after transplantation. Our aim is to understand the relationship between satellite cells-derived muscle precursor cells (MPCs) and NLBs using an *in vitro* co-culture model: this will be useful in perspective of a tissue engineering approach for bowel regeneration and

skeletal muscle. Our records highlighted that NLBs were able to form new myotubes in presence of MPCs. Co-cultures in myogenic medium showed a remarkable improvement of MPCs differentiation by NLBs, promoting the formation of sarcomeric striatures onto myotubes and increasing the desmin expression of MPCs. On the other side, using neurogenic medium MPCs-NLBs showed a neural-like phenotype. As future perspectives, we need to understand the relationship between MPCs and NLBs and if the synapses are involved in this process; to verify if the seeding on a biocompatible polymer influences the behaviour of neural cells; and we must confirm these data with an *in vivo* skeletal and smooth muscle differentiation.

We have finally explored the possibility of deriving smooth muscle cells from a different source, taking in consideration the difficulties related to the expansion of both skeletal and smooth muscle progenitors. Therefore, we aim to derive functional smooth muscle cells (SMCs) from non-muscle cells, such as human Amniotic Fluid Stem (hAFSC) cells. hAFSC were transduced using vector encoding ZsGreen under the αSMA promoter. SMhAFSC expressed significantly higher level of smooth muscle genes (such as αSMA, desmin, calponin and smoothelin expression) after selective culture condition. These features were confirmed by immunofluorescence, demonstrating a single lineage commitment; TEM established increased intermediate filaments, dense bodies and glycogen deposits in SMhAFSC, similar pattern compared to SMCs; and sequential imaging analyses demonstrated that SMhAFSC have a higher contractile potential than hAFSC. Consecutive single cell sampling showed the presence of voltage-dependent calcium activated potassium channels on differentiated SMhAFSC and showed a higher production of carbon dioxide. In conclusion, we were able to generate to functional SMCs starting from a non-muscle precursor; secondly the transduction process may represent a valuable tool to select SM committed population. This step may eventually overcome the well-known problem of expanding SM progenitors, making these cells amenable to tissue engineering.

Sommario

Il nostro gruppo ha recentemente caratterizzato due distinte popolazioni di cellule satelliti, classificate come cloni a bassa proliferazione (LPC) e ad alta proliferazione (HPC), che si differenziano in termini di proliferazione, potenziale rigenerativo e metabolismo mitocondriale. Nel mio lavoro di dottorato, abbiamo valutato e caratterizzato la loro biologia cellulare con particolare attenzione a quelle differenze intrinseche presenti anche prima della loro clonazione. Infatti, ambo le tipologie clonali possono essere distinte mediante il potenziale di membrana mitocondriale ($\Delta\Psi_m$) subito dopo l'isolamento dalla fibra. Questo dato è in accordo con lo stato ossido riduttivo mitocondriale misurato tramite NAD^+/NADH e la quantificazione della produzione di CO_2. Questi risultati sono responsabili delle differenze metaboliche e possono essere spiegati dalla diversa espressione dell'enzima glicolitico Pfkfb3. Inoltre la concentrazione mitocondriale del Ca^{2+} e la sensibilità all'apoptosi sono modificate così come la dimensione della rete mitocondriale. In conclusione, siamo stati in grado di determinare quale clone rappresenta la cellula staminale all'interno della popolazione di cellule satelliti. Queste nuove osservazioni sperimentali rivelano caratteristiche fisiologiche della biologia delle popolazioni delle cellule satelliti prima e dopo la clonazione, mettendo in luce un'eterogeneità intrinseca della cellula satellite.

Nella seconda parte della mia tesi abbiamo esplorato la possibilità che le cellule satelliti possano, se opportunamente stimolate, trans-differenziarsi in cellule muscolari lisce. Il sistema nervoso enterico normalmente interagisce con le cellule muscolari per controllare l'attività peristaltica e secretoria della parete intestinale. L'incompleta colonizzazione dell'intestino da parte delle cellule della cresta neurale provoca la malattia di Hirschsprung, caratterizzata da aganglionosi del colon distale. Le neurosfere (NLBs), precursori enterici in grado di auto-rinnovarsi, possono generare neuroni e glia; essere isolate dall'intestino di topi, ratti e umani e sono in grado di colonizzare l'intestino dopo il trapianto. Il nostro obiettivo è di capire la relazione tra i precursori di cellule satelliti (MPCs) e NLBs utilizzando un

modello *in vitro* di co-coltura: questo sarà utile in prospettiva di un approccio di ingegneria tissutale per la rigenerazione intestinale e muscolo scheletrico. I nostri dati hanno evidenziato che NLBs, in presenza di MPCs, sono in grado di formare nuovi miotubi. L'uso di terreni di coltura miogenici ha evidenziato un notevole aumento della differenziazione in senso muscolare, promuovendo la formazione di striature ed aumentando l'espressione di desmina. Dall'altra parte, l'utilizzo di terreni di coltura neurogenici ha mostrato un fenotipo simil neurale. Come prospettive future, dobbiamo comprendere ulteriormente la relazione tra MPCs e NLBs e se le sinapsi sono coinvolte in questo processo; si deve verificare se un loro utilizzo su polimeri biocompatibili ne possa influenzare il comportamento, ed infine è necessaria una conferma dei suddetti dati tramite un'analisi di differenziazione *in vivo* in muscolo scheletrico e liscio.

Nella terza ed ultima fase del mio lavoro, ci siamo focalizzati ad esplorare la possibilità che cellule non-muscolari possano, se opportunamente stimolate, differenziare in senso muscolare liscio. Il nostro obiettivo è stato quello di ottenere cellule muscolari lisce (SMCs) partendo da cellule staminali del fluido amniotico umano (hAFSC). hAFSC sono state trasdotte utilizzando un virus codificante per ZsGreen sotto il promotore αSMA. SMhAFSC così ottenute hanno evidenziate un alto livello d'espressione dei geni del muscolo liscio (come αSMA, desmina, calponina e smoothelin). Queste caratteristiche sono state confermate da molteplici analisi: di immunofluorescenza, dimostrando la positività a marcatori specifici per il muscolo liscio; microscopia a trasmissione elettronica (TEM), dove si verificava l'aumento della presenza di filamenti intermedi, di corpi densi e depositi di glicogeno, modello simile rispetto alle SMCs. Analisi in time-lapse di SMhAFSC hanno dimostrato che queste possiedono un potenziale contrattile superiore rispetto hAFSC e studi su singola cellula hanno evidenziato la presenza di canali calcio voltaggio-dipendenti attivati da potassio solamente su SMhAFSC. In conclusione, siamo stati in grado di generare di cellule muscolari lisce funzionali da un precursore non-muscolare ed in secondo luogo il processo di trasduzione può rappresentare un valido strumento per distinguere e selezionare differenti popolazioni.

Questa fase può eventualmente superare il ben noto problema dell'espansione di progenitori di cellule muscolari lisce, rendendo queste cellule suscettibili per approcci d'ingegneria tessutale.

Chapter I

1. Introduction

1.1 Regenerative medicine

Regenerative medicine is focused on the repair, replacement and regeneration of cells, tissues or organs to restore impaired function resulting from any cause (Daar et al., 2007). Major advances have been permitted by the discovery and isolation of stem cells that harbour the capacity for self-renewal and the potential to differentiate into one or more types of specialized cells (Mimeault et al., 2008). Not only the stem cell-potential but also the appropriate route of cell administration to a damaged/developing organ is an essential prerequisite for the success of cell engraftment and organ repair. It is estimated that congenital disease are responsible for over ⅓ of all paediatric hospital admissions and for up to 50% of the total cost of paediatric hospital treatment (McCandless et al., 2004). Through the improvement of the medical care, these patients can now survive to adulthood requiring possible therapeutic treatments include therapy with stem cells, gene transfer or combined gene therapy stem cell approach. This is potentially achievable by deriving stem cells with pluripotent ability from different sources; one of the most promising is the amniotic fluid (Shaw et al., 2011).

Moreover, regenerative medicine may overcome the need of organs for transplantation, which is continuously increasing. The number of these patients is in fact far exceeds the organ supply, and organ shortage is expected to worsen as the aging population increases. In this case, the goal of regenerative medicine is to replace or restore normal function of cells, tissues and organs that are damaged by disease or after injury. Regenerative medicine strategy fall into three categories:

1. Cell based therapy.
2. Use of biomaterial alone (scaffold).
3. Use of scaffold seeded with cells.

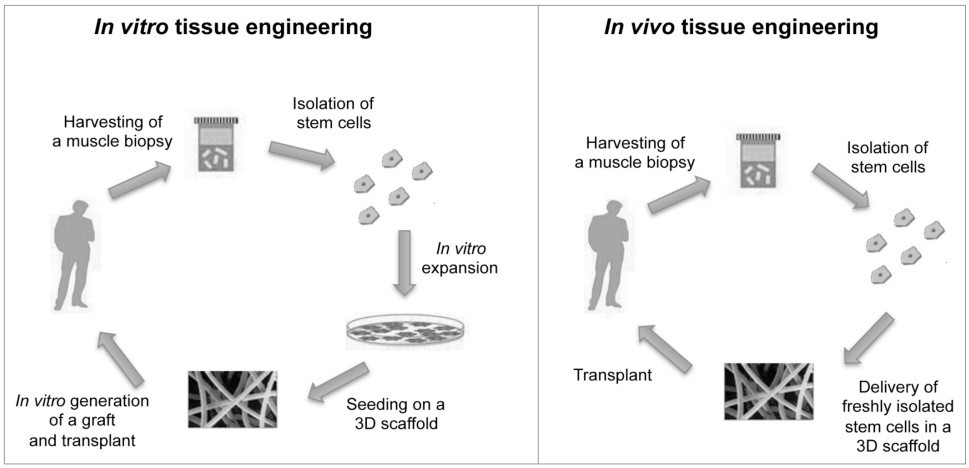

Figure 1: These cartoons explain the differences between the approaches of in vitro and in vivo tissue engineering. In vitro tissue engineering (left): a muscle biopsy is collected from an individual, stem cells are isolated and then expanded through cell culture techniques; they are then seeded on a 3D scaffold and a graft is generated and then transplanted. In vivo tissue engineering (right): a muscle biopsy is collected from an individual, then stem cells are isolated and immediately delivered on a 3D scaffold, that is promptly transplanted (from Rossi et al., 2010).

Cells used for tissue engineering are usually obtained from a small biopsy of tissue, expanded *in vitro*, seeded onto a matrix, and implanted back into the host. The crucial point is the biopsy source because the donor tissue can be allogenic (donor derived) or autologous (the host's cells). The latter is ideally the best option for transplantation because cells are not rejected by the immune system, so the immunosuppressant drugs are avoided. In spite of this, inherent difficulty of *ex vivo* expansion is a key limiting factor. Even if some organs, such as the liver, have a very high regeneration rate *in vivo*, cells from these organs can be difficult to expand *in vitro* (Hipp et al., 2008).

1.2 Skeletal muscle – Structure & Function

Skeletal muscle is constituted by cylindrical multinucleated cells, called muscle fibers, bundled together and wrapped by connective tissue. Three connective tissue layers can be distinguished in skeletal muscle and these form the lattice network: the *epimysium* is the deep fascia component and it is contiguous with the tendon and endosteum (fascia surrounding bone). The *perimysium* unsheathes individual muscle fibers into fascicules (bundles). The *endomysium* is located between fibers and it unsheathes single myofibres. Within the muscle cell, the major intracellular source of calcium needed for muscle contraction is the sarcoplasmic reticulum, which

connects to the transverse (T) tubules that surround the sarcomeres (Figure 2).

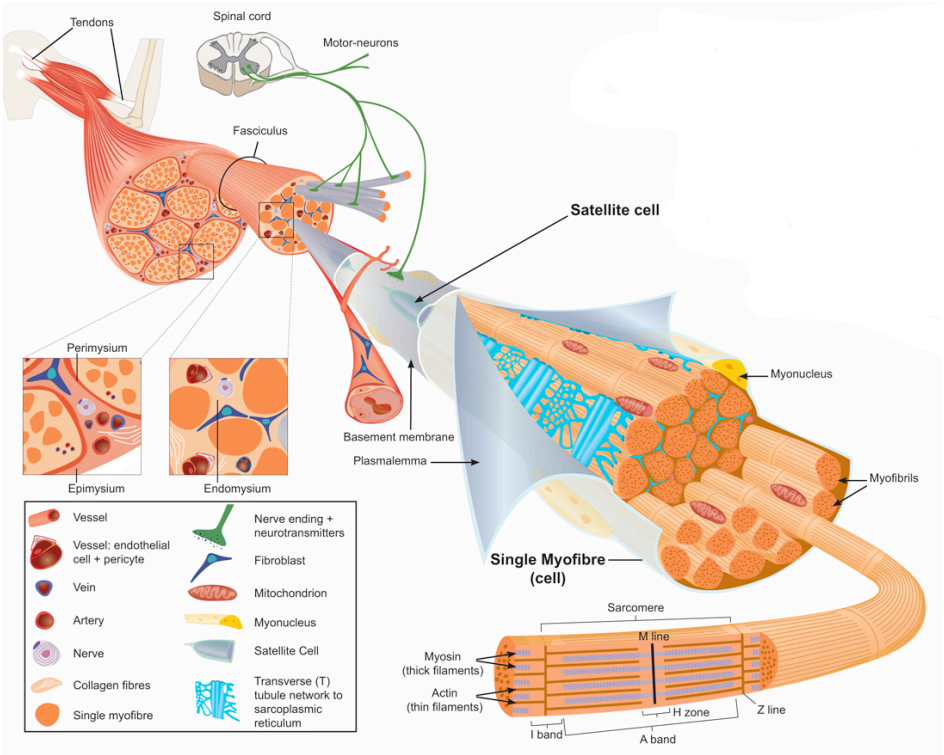

Figure 2: Scheme of skeletal muscle and associated structures. Satellite cells are located under the basal lamina of the myofiber (Modified from Tajbakhsh S, 2009).

The nuclei are located at the periphery of the muscle cells, just under plasma membrane (sarcolemma), while closed to them and surrounded by their own membrane, are present the nuclei of satellite cells, the skeletal muscle stem cells.

The contractile proteins organized in myofibrils fill cytoplasm of muscle cells. Each myofibril runs the entire length of the fiber. In transversal section, myofibrils display a characteristic-banding pattern of striated skeletal muscle. This aspect is owing to the lined up in series of sarcomeres, that are the structural units. The sarcomere comprises two sets of filament: thin ones, made mostly of actin, and thick filaments, made mostly of myosin. Several other important proteins, like troponin and tropomyosin, nebulin, and desmin, help to hold these units together (Charge et al., 2004).

1.3.1 Skeletal muscle – Muscle stem cells

Satellite cells (SCs) are the skeletal muscle stem cells, first described in frog muscle by Alexander Mauro in 1961 (Mauro A, 1961). Characterized by their morphology and position relative to mature myofibres, during muscle

development, SCs adhere to the surface of myotubes prior to the formation of the basal lamina, such that the basal lamina surrounding the myofiber is a continuous (Armand et al., 1983).

Their roles are to mediate the postnatal growth of muscle, constitute the primary means by which the mass of adult muscle is formed, and being responsible for the postnatal growth and regeneration in adult skeletal muscle. SCs reside beneath the basal lamina of myofibres and comprise 2 – 7% of the nuclei associated with a specific fiber (Sambasivan et al., 2007). In adult undamaged muscle, SCs are normally quiescent but they are activated to enter the cell cycle in response to an injury. MPCs (Myogenic Precursors Cells), the progeny of activated SCs, undergo multiple rounds of division before fusion in myotubes and new myofibres (Rosenblatt et al., 1994). Activated satellite cells also generate descendants that restore the pool of quiescent satellite cells (Kuang et al., 2008b).

About 32% of muscle nuclei are coming from SCs at birth, whilst in the adult there is a drop to less than 5% suggesting the direct reflection of SC fusion into new or pre-existing myofibres (Bischoff R, 1994). Their number, in normal physiological conditions, remains constant, over multiple cycles of degeneration/regeneration, demonstrating a capacity for self-renewal. Although in pathological conditions, such as DMD, the number and the doubling potential of SCs become severely reduced, presumably due to high levels of ongoing regeneration (Emery E, 1998).

1.3.2 Myogenic regulatory factors in satellite cell proliferation and differentiation

The primary myogenic regulatory factors (MRFs) are Myf5, MyoD, myogenin, and MRF4. The first two are required for the determination of myoblasts, whereas the others are involved in the regulation of terminal differentiation (Charge et al., 2004).

The majority of quiescent SCs in the mouse express low levels of Myf5, most are positive for Pax7, M-cadherin, CD34, and do not express myogenic regulatory factors of the MEF2 family or other known markers of terminal differentiation. Activated SCs are positive for MyoD, and negative for Msx1 and Nestin, whereas in quiescent SCs there is the opposite pattern.

Both are positive for Pax7, Sox8/9, Myostatin and Myf5.

In terms of cell surface markers, Caveolin-1 (cell-cycle arrest), CTR (regulates quiescent state) and Sphingolmyelin (cell-cycle entry) are present in quiescent SCs but not after activation, while Necdin (that promotes differentiation) and ErbB receptor (anti-apoptotic function) are exclusively present in the activated state (Kuang et al., 2008a). SCs express Vascular Cell Adhesion Molecule 1 (VCAM-1), c-met (receptor for Hepatocyte Growth Factor, HGF), Neural Cell Adhesion Molecule 1 (NCAM1), Foxk1, CD34, and Syndecans 3 and 4. Moreover, in Rudinicki's laboratory, several additional novel genes were identified: IgSF4, Neuritin, Hoxc10, TcR-β, Klra18, Itm2α, G0S2, and Megf10 that are expressed in satellite cells *in vivo* but are not expressed by primary myoblasts (Seale et al., 2004).

In addition, numerous growth factors such as FGF6, HGF, BMPs and NO have been suggested to have roles in stimulating SCs activation. Nevertheless, the precise molecular mechanisms regulating their functions remain poorly understood. It has been reported that some of these markers are expressed at different levels between quiescent and activated SCs (Jankowski et al., 2002).

In humans, SCs markers do not fully correspond to those in the mouse. CD34 does not mark satellite cells in human muscle, and M-cadherin is not so consistent a marker of human as of mouse satellite cells. Among the more reliable markers of satellite cells in human muscle is neural cell adhesion molecule (CD56), which also marks lymphocytes that may enter degenerating muscle in large numbers (Péault et al., 2007).

1.3.2.1 The myogenic networks – PAX3/7

The paired-box family of transcription factors (Pax1 – 9) has important functions in the regulation of the development and differentiation of diverse cell lineages during embryogenesis.

Pax7 and the closely related Pax3 gene are paralogs with almost identical amino-acid sequences and partially overlapping expression patterns during mouse embryogenesis. These proteins bind similar sequence-specific DNA elements, suggesting that they regulate similar sets of target genes. Analysis of null-mice indicates that they are required for the development of a

number of distinct cell lineages and appear to have non-redundant roles in myogenesis (Seale et al., 2004).

Pax3$^{-/-}$ model, *Splotch (Sp)* mice, do not survive to term and fail to form limb muscles due to impaired migration of Pax3-expressing cells originating from the somite. Moreover compound mutant *Sp/Myf5*$^{-/-}$ mice do not express MyoD in their somites, suggesting that Myf5 and Pax3 function upstream of MyoD in myogenic determination. As a result, Pax3 was suggested to function as an indirect upstream factor that induced migration or other cellular changes to facilitate subsequent induction of MyoD transcription. It also mediates the migratory phase of the lineage, whereas its paralog gene is required to achieve their myogenic potential. Pax3 rules the regulation of the developmental program of MyoD-dependent migratory myoblasts.

On the other side, Pax7 is specifically expressed in SCs in adult muscle, and their daughter precursor cells *in vivo* and primary myoblasts *in vitro*. Pax7$^{-/-}$ mice and have confirmed the progressive ablation of the SCs lineage in multiple muscle groups (Seale et al., 2000). SCs lost is in part due to apoptosis implying this factor in survival of SCs. Small Pax7-deficient cells do survive in the SCs position, but these cells arrest and die upon entering mitosis. Muscles collected from Pax7$^{-/-}$ mice are reduced in size, the fibers contain approximately 50% the normal number of nuclei and fiber diameters are significantly reduced. These data confirm the essential role for Pax7 in regulating the myogenic potential of SCs (Kuang et al., 2006). Furthermore, Bajard and colleagues recently demonstrated that Pax7 binds a 57-kb regulatory element upstream of the Myf5 transcription start site (Bajard et al., 2006).

In conclusion, Pax3 is critical for survival of stem cell in embryo whereas Pax7 is necessary for satellite cell in adult (Punch et al., 2009).

1.3.2.2 The myogenic networks – The myogenic regulatory factors (MRFs)

MRFs form a group of bHLH transcription factors (MyoD, Myf5, myogenin, MRF4). MRF proteins contain a conserved basic DNA-binding domain that binds the E box, a DNA motif that contains the core E-box sequence CANNTG. Time-scale of MRFs expression is:

- MyoD is up regulated shortly after induction of differentiation followed by myogenin.
- Myf5 and MyoD levels progressively decrease after this point.
- The levels of myogenin increase through differentiation.
- Followed by up-regulation of MRF4 several days after the induction of differentiation as myogenin levels decrease.

The Mef2 class of transcription factors also has an important regulatory role in the control of muscle-specific transcription. In addition, Mef2 proteins and MRFs synergistically co-activate E-box- and Mef2-site-containing promoters.

1.3.2.3 The myogenic networks – MyoD vs Myf5

Mice lacking MyoD gene display no overt abnormalities in muscle but express about fourfold higher levels of Myf5 (Rudnicki et al., 1992), whilst embryos MyoD$^{-/-}$ display normal development of paraspinal and intercostal muscles in the body proper; muscle development in limb buds and branchial arches is delayed by about 2.5 days. Although MyoD$^{-/-}$ embryos exhibit delayed development of limb musculature, the migration of Pax-3-expressing cells into the limb buds and subsequent induction of Myf5 in myogenic precursors occur normally (Rudnicki et al., 2008).

In contrast, newborn Myf5-deficient animals are also viable and display apparently normal muscle (Braun et al., 1992) and embryos lacking Myf5 display normal muscle development in limb buds and branchial arches and a marked delay in development of paraspinal and intercostal muscles.

Double knockout for Myf5 and MyoD strongly supports the notion that the putative myogenic lineages that give rise to epaxial and hypaxial musculature have different requirements for Myf5 or MyoD for appropriate development. Thus, Myf5 and MyoD are required for the determination of myogenic precursors and act upstream of myogenin and MRF4. These results indicate that Myf5 expression in the limb is insufficient for the normal progression of myogenic development (Rudnicki et al., 2008).

1.3.2.4 The myogenic networks – MRF4 and Myogenin

MRF4$^{-/-}$ mice display a range of phenotypes consistent with a late role for MRF4 in the myogenic pathway. MRF4 function may be substituted by the presence of myogenin but only in the presence of MyoD. Notably, MRF4 appears to have a role as a determination factor in a subset of myocytes in the early somite and as a differentiation factor in later muscle fibers.

On the other hand, mice lacking myogenin are immobile and die perinatally due to deficits in myoblast differentiation, as evidenced by an almost complete absence of myofiber (Rudnicki et al., 2008).

1.3.3 Skeletal muscle regeneration

Skeletal muscle degenerates after an injury or during disease. Throughout the myofibres necrosis, three different phases characterize the regeneration process (Tajbakhsh S, 2009):

1. Inflammation.
2. Tissue reconstruction.
3. Tissue remodelling.

SCs population is heterogeneous based on the expression of two transcription factors: Pax7 and Myf5. Genetic analysis revealed that satellite cells divide through apical-basal-oriented cell division where the apical Pax7^{+}/Myf5^{+} cell undergo terminal differentiation (committed progenitors) and the basal one Pax7^{+}/Myf5^{-} contribute to satellite cells reservoir (Kuang et al., 2007; Punch et al., 2009).

Furthermore SCs possess different myogenic program depending on MyoD and Myf5 expression. Whereas MyoD is up regulated, the program show early differentiation (analogous to the Myf5-null condition). In contrast, an up-regulation of Myf5 brings an enhanced proliferation and delayed differentiation (as in MyoD-null behaviour) (Rudnicki et al., 2008). A schematic illustration is depicted in figure 3.

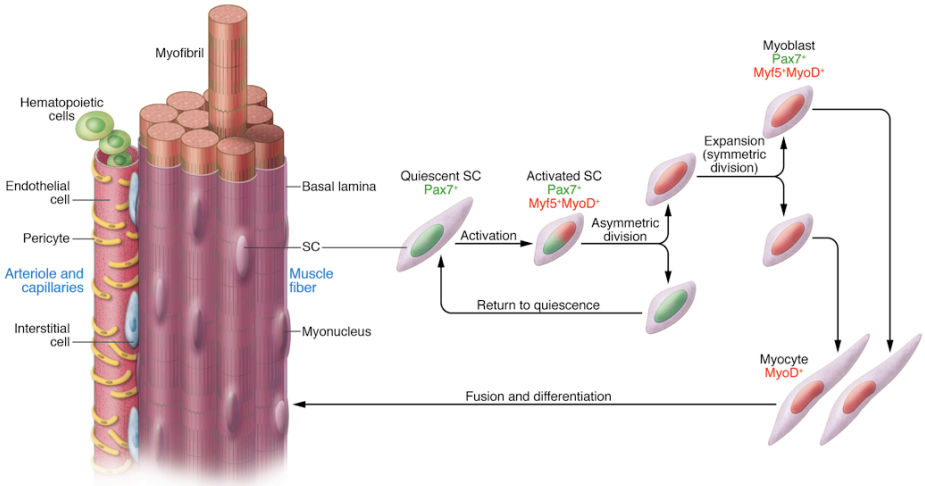

Figure 3: Asymmetric cell division during activation of SCs. This is a drawing representing the SC activation *in vivo*: Pax7, MyoD and Myf5 being expressed in differentiating cells and Pax7 in cells returning to quiescence in order to maintain a pool of progenitors (from Tedesco et al., 2010).

1.3.4 Mechanisms of satellite cell division

Asymmetric and symmetric cell divisions can direct self-renewal and lineage progression. The first one is associated with tissue homeostasis and a linear mode of cell expansion whereas symmetric division results in exponential cell growth. Interestingly, Morrison and colleagues found that regulators of asymmetric division have a propensity to be tumour suppressors whereas those regulating symmetric division are oncogenes (Morrison et al., 2006). This hierarchical composition of differentiating progenitors and self-renewable stem cells assures the extraordinary regenerative capacity of skeletal muscles.

There are three different models of asymmetric division in SCs (Kuang et al., 2008b):

1. Asymmetric co-segregation of older and newer template DNA strand into daughter cells: the daughter cell that inherits the older template DNA strands also expresses Sca1, suggesting a self-renewing fate; the other one that inherits the newer template DNA strands co-expresses desmin, indicating a committed fate.
2. Numb-mediated asymmetric divisions: during mitosis, Numb protein is segregated to one pole and therefore inherited by one daughter cell. However, it is unclear whether the daughter cell that inherits Numb subsequently self-renews or differentiates (Kuang et al., 2008b).
3. Asymmetric self-renewal of $Pax7^{+}/Myf5^{-}$ satellite cells: apical-basal-

oriented divisions give rise to a self-renewed $Pax7^{+}/Myf5^{-}$ and a committed $Pax7^{+}/Myf5^{+}$ daughter cell (that expresses higher levels of Delta1).

Numb/Notch signalling pathways are involved in stem cells behaviour. Delta1 stimulates Notch signalling leading satellite cells mobilization in adult muscles. Megf10, a transmembrane protein, was found as a novel marker for quiescent and activated SCs, and also has been proposed to be involved in SCs proliferation (Holterman et al., 2007). Notch signalling regulates the balance between progenitor cell self-renewal and myogenic differentiation. Moreover, Wnt signalling plays role in promoting myogenesis during embryogenesis. Canonical signalling activates early transcription of Myf5 in the somites (Borello et al., 2006) while non-canonical signalling promotes Pax3 activity (Brunelli et al., 2007). In conclusion, Notch signalling supports proliferation of SCs, and Wnt signalling carries out terminal differentiation (Nagata et al., 2006).

In this matter, the niche directs the maintenance of stem cell identity, the asymmetric division and issue of committed daughter cells (Kuang et al., 2008b). It has been hypothesized that cell polarity could be established within the niche by cell-cell interactions mediated by cadherins and cell-extracellular matrix interactions mediated by integrins (Rudnicki et al., 2008). Indeed, the basal lamina side of SCs expresses integrin α7β1 receptors that interact with laminin whereas the apical side expresses the cell adhesion molecule m-cadherin. The asymmetric distribution of cell surface receptors and adhesion molecules in response to differential apical-basal niche signals forms a structural basis for cell polarity (Kuang et al., 2008b).

1.3.5 Skeletal muscle cell niche

SCs are localized under the basal lamina along the surface of muscle fibers. The satellite cell niche is asymmetric in nature: one side of cell is in contact with the plasmalemma and on the other side with the basement membrane (Tajbakhsh S, 2009). The stem cell niche is the microenvironment within every stem cell resides and it is determined by:

1. Molecular signals derived from the myofiber.

2. Extracellular matrix.
3. Microvasculature.

Mechanical, electrical and chemical signals from the host fiber have all been shown to be involved in the regulation of SC function (Charge et al., 2004). Moreover the components of the extracellular matrix are important, such as proteoglicans, collagen and laminin. Interactions between myofiber and SCs could me mediated by Ca^{2+} dependent adhesion molecule m-cadherin. However, in adult muscle its expression is limited, and SCs function appears to be unaffected in m-cadherin-null mice. Nevertheless, the mechanism behind the influence of the myofiber on its SCs remains unexplored (Hollnagel et al., 2002).

It has been proposed that also the vasculature could be an integral component of the satellite cell niche since over 95% of SCs have been reported to be subjacent to an endothelial cell (Christov et al., 2007). In humans and mice, 68% and 82% of SCs, respectively, are found to be localized within 5 mm from neighbouring capillaries or vascular endothelial cells, under both quiescence and proliferation states. Extrinsic signals from the circulatory system and interstitial cells are relayed to SCs through the basal lamina. These anatomical features of their niche suggest that a combination of signals from the host muscle fiber, circulation system and ECM govern the quiescence, activation and proliferation of SCs (Kuang et al., 2008a).

1.3.6 Satellite cell self-renewal

The mechanism by which SCs undergo self-renewal in adult skeletal muscle is still poorly understood. However, it is known that the balance between self-renewal and differentiation is crucial for stem cell maintenance and tissue homeostasis. Dysfunction leading to decreased self-renewal would eventually lead to depletion of the stem cell population (as in Duchenne Muscular Dystrophy), while uncontrolled self-renewal would result in overproduction of stem cells and potentially tumorigenesis.

One mechanism to achieve this balance is through asymmetric divisions that generates two unequal daughter cells: the first destined to self-renew and the second to differentiate. On the other hand, through a stochastic self-renewal

process identical daughter cells can be generated by symmetric divisions and afterward adopt distinct fates stochastically. Alternatively, a modified stochastic self-renewal may occur, in which some stem cells exclusively generate self-renewing daughters whereas others generate differentiating daughters, so that a stable stem cell number is maintained (Kuang et al., 2008a).

John Cairns proposed in 1975 the "immortal DNA strand" hypothesis, in which he explained a possible mechanism for adult stem cells that minimize mutations. Instead of a random segregation during mitosis, stem cells divided their DNA asymmetrically retaining a template set of DNA strands in each division (parental strands). By preserving the same set of DNA, adult stem cells would avoid mutations arising from errors in DNA replication, reducing their rate of accumulation of mutations that could lead to genetic disorders such as cancer (Cairns J, 1975). Consistent with this hypothesis, Conboy and colleagues demonstrated via BrdU pulse-chasing experiments that all the older template DNA strands are co-segregated into the self-renewing daughter cells ($Sca1^+$) whilst all the younger template DNA strands are co-segregated into the differentiating daughter cells $desmin^+$ (Conboy et al., 2007). Because asymmetric DNA strand segregation only occurs in a fraction of SCs, currently the question remains whether DNA co-segregation is a constitutive property of a primitive subpopulation of SCs that maintains the homeostasis of their niche. If this is true, it will be of interest to identify the unique molecular markers of these cells.

Another point is that Numb-mediated asymmetric divisions have been observed during SCs proliferation. Asymmetric distribution of cytoplasmic Numb into one pole of a dividing myoblast is associated with cell fate determination of the daughter cells that have inherited Numb also received all the older template DNA strands (Shinin et al., 2006), suggesting they are the self-renewing cells according to the immortal DNA strand hypothesis. However, Numb has also been shown to be asymmetrically segregated into the differentiating daughter myoblasts (Conboy et al., 2002), consistent with its role in repressing Notch. This obvious discrepancy may be due to differences in the cell-cycle phase during which the observations were

made, as the subcellular localization and function of Numb vary throughout the cell cycle (Zhou et al., 2007).

Thirdly, Kuang and colleagues demonstrated that a non-committed $Pax7^{+}/Myf5^{-}$ SCs could asymmetrically generate a self-renewal ($Pax7^{+}/Myf5^{-}$) and a committed ($Pax7^{+}/Myf5^{+}$) daughter cell *in vivo* (Kuang et al., 2007). This asymmetric cell fate segregation is the direct result of an asymmetric division. Moreover, these results suggest that $Pax7^{+}/Myf5^{-}$ SCs have never activated Myf5 during proliferation, as opposed to the stochastic self-renewal model that would predict an initial up-regulation of Myf5 in all activated proliferating cells and followed by self-renewal through down-regulation of Myf5, indicating that opposing signalling pathways must be present in the two daughter cells that function to activate or repress Myf5 gene expression. In conclusion, these data support the notion that asymmetric division and signals within SCs niche co-operate to regulate their self-renewal. However, there are evidences that suggest a role for Myf5 in facilitating SCs self-renewal. In particular, expression of Myf5 alone may facilitate stem cell self-renewal within the context of skeletal muscle. Cornelison and colleagues revealed that activated SCs first express either Myf5 alone or MyoD alone, prior to co-expressing Myf5 ad MyoD and subsequently progressing through the myogenic program suggesting that expression of Myf5 may define a developmental stage during which SCs undergo self-renewal (Cornelison et al., 1997).

Importantly, none of the above models are mutually exclusive and all could coexist to maintain the steady-state numbers of SCs.

1.3.7 Origin of satellite cells

Post-natal growth of the muscles is accomplished by satellite cells and in adult they maintain homeostasis of the muscle tissue. The embryological origin of satellite cells was first addressed in a chick-quail chimera study. Electroporation of the central dermomyotome in the trunk with a molecular marker showed that virtually all of these marked cells gave rise to $Pax7^{+}$ SCs after hatching, thereby establishing the dermomyotome origin of SCs, in chick (Armand et al., 1983).

In the same year, two different groups explained that SCs originate from the

Pax3^{+}/Pax7^{+} cells in the mouse somites (Kassar-Duchossoy et al., 2005; Relaix et al., 2005). The ventral lips of limb level somites give rise to both migratory endothelial progenitors expressing VEGFR2 and muscle progenitors marked by Pax3 expression. This raises the possibility of an endothelial progenitor contribution to the SCs pool. However, Sambasivan and colleagues proved that SCs in the limb arise from the Pax3^{+} cells in the hypaxial somites (Sambasivan et al., 2007).

In newborn animals the proportion of SCs is higher and they proliferate to add nuclei to the growing muscle. The time window in which quiescent SCs appear, and the mechanism by which this quiescent pool is set apart from the progenitors that participate in postnatal growth is not known (Sambasivan et al., 2007).

Quiescent SCs adjacent to mature fibers express c-Met and M-cadherin proteins but do not express markers of committed myoblasts, such as Myf5, MyoD or desmin (Irintchev et al., 1994; Cornelison et al., 1997). Committed myoblasts would therefore be generated as a function of their microenvironment, and available growth factors. Such a model is also consistent with the observed ability of adult muscle-derived stem cells to repopulate the hematopoietic compartment as well as to give rise to skeletal myocytes following intravenous injection into irradiated mice (Ferrari et al., 1998; Gussoni et al., 1999).

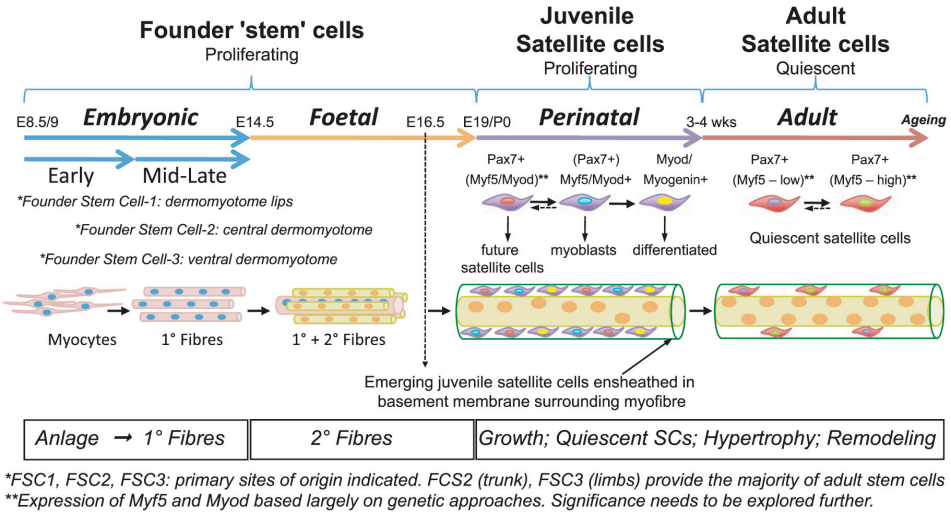

Figure 4: Scheme of skeletal muscle development and homeostasis in vertebrates. Multiple phases of growth mobilize stem and progenitor cells to establish skeletal muscles. It is proposed that FSC1 will be largely exhausted in the embryo will give rise to the majority of adult SCs. Founder stem cells (FSC1, FSC2, FSC3) (from Tajbakhsh S, 2009).

1.3.8 Clinical approach

The original report that cultured myoblasts can restore dystrophin expression in *mdx* mice (mouse model for Duchenne Muscular Dystrophy) stimulated great enthusiasm in clinical trials in muscular dystrophies (Kuang et al., 2008a). Indeed, autologous SCs-derived myoblasts have been used in various clinical trials towards cardiac repair, some with promising results (Menasche P., 2007).

SCs present several advantages. First of all, they are one of the few adult stem cells that can be identified by anatomical localization. Secondly, their efficient myogenic differentiation and self-renewal properties ensure transplantation. In addition, SCs are so far the most efficient cells capable of spontaneous myogenic differentiation and muscle repair. *In vitro* culture conditions are well established, and the accessibility from muscle biopsies is an easy procedure.

However, SCs are not suitable for systemic delivery. Currently, their progenitors are only suitable for intramuscular injections, a procedure that is laborious and less tolerable by patients. Nonetheless, SCs possess poor migration and poor survival after transplantation, so myoblasts need to be injected at multiple sites at very high density requiring repeated injections. Furthermore, after culture, SCs reduce myogenic potential: their *in vitro* expansion is necessary because a large number of myoblasts are required for each patient. In spite of this, recent studies in mice indicate that cultured satellite cells are far less efficient in cell-based therapy (Rossi et al., 2011).

Nevertheless, several hurdles greatly slowed efforts to control the great potential of stem cell-based therapy for muscular dystrophies because autologous SCs cannot produce dystrophin. Anyway, there are several potential remedies to this problem:

1. Recent studies suggest that the capability of intramuscular migration of freshly isolated satellite cells is much higher as compared with cultured myoblasts (Montarras et al., 2005).
2. The use of micro-scaffolds improves the migration of myoblasts greatly after implantation (Hill et al., 2006).
3. Matrix metalloproteinase treatment improves myoblast migration and muscle healing (Bedair et al., 2007).

4. Hydrogel (hyaluronic acid-based scaffold) could increase satellite cell viability during cell therapy (Rossi et al., 2011).

A final possibility is to explore the feasibility of the systemic delivery of fresh or cultured satellite cells.

Fundamental cell biology sets the differences between Satellite Cells clones

1.4.1 Background

Satellite cells are closely associated with skeletal muscle fibers since they are intimately involved in their homeostasis, mediating essential processes of repair (Biressi et al., 2010) and defects in SCs lead to muscle pathologies (Gayraud-Morel et al., 2009; Sambasivan et al., 2007; Shi et al., 2006). In adult skeletal muscle, SCs reside beneath the basal lamina of muscle, representing 2-7% of the nuclei associated with a fiber (Bischoff R, 1994; Tedesco et al., 2010). SCs are mitotically quiescent, and activated (i.e., enter the cell cycle) in response to several stimuli such as: stretching, injury or electrical stimulation. The descendants of activated SCs, called MPCs (Myogenic Precursor Cells) or myoblasts, undergo multiple rounds of division before fusion into newly formed myotubes. Charge and colleagues demonstrated that SCs are distinct from their daughter myogenic precursor cells by biological, biochemical and genetic criteria (Charge et al., 2004) while, on the other hand, activated SCs could restore the SCs pool (Charge et al., 2004; Kuang et al., 2008b; Tedesco et al., 2010).

At the beginning of their studies, SCs were considered unipotent stem cells (hence possessing the ability of generating just a single phenotype) whilst, in the last years, it was clearly demonstrated that opposite differentiation towards osteogenic (Huang et al., 2010) and adipogenic pathways (Sambasivan et al., 2007) was possible too. However, even though the pool of SCs is accepted as the major, and possibly, the only source of myonuclei in postnatal muscle, it is likely SCs are not all multipotent stem cells (Appell et al., 1988; Rosenblatt et al., 1994; Schultz E, 1985).

Thus, evidences for diversities within the myogenic compartments have been described both *in vitro* and *in vivo*. Alternative sensitivity to high-dose irradiation revealed that at least two populations of SCs are present that can be recognized by proliferative and myogenic capacities within a proportion that varies according to the age (Biressi et al., 2010).

As we previously described (Rossi et al., 2010), in rat muscles there are two subpopulations of SCs, coexisting in fixed proportions on the single fiber and distinct in term of their proliferative capacity. One is called Low Proliferative Clone (LPC), with myogenic fate, and the other High Proliferative Clone (HPC), that spontaneously produced adipocytes.

In this study, we showed how these two clones possess different myogenic gene expression and interestingly distinctive metabolism. Namely, we recorded differences in functional parameters for mitochondrial physiology such as: mitochondrial membrane potential ($\Delta\Psi_m$), ATP production and Reactive Oxygen Species (ROS) generation that rendered the proliferative clones to be more glycolytic compared to the low ones. Here, we endeavoured to address their cell biology in greater length and therefore addressed their NADH redox state, cellular CO_2 production, expression of key metabolic pathways together with mitochondrial Ca^{2+} signalling and mitochondrial dependent apoptosis (Campanella et al., 2009; Gastaldello et al., 2010). Most notably, differences at clonal level are recapitulated in the un-cloned state.

1.4.2 Materials and Methods

Animals

Three to four month-old Sprague-Dawley wild type rats (Harlan, Indianapolis, U.S.A.) were used in this study. Animal care and experimental procedures were performed in accordance with ‘‘D.L. 27-1-1992, number 116, applicative declaration of Healthy Minister number 8 22-4-1994’’.

Isolation of Single Fibers from Extensor Digitorum Longus (EDL) and *Soleus* Muscles

Single muscle fibers with associated SCs were isolated from *extensor digitorum longus* (EDL) and *soleus* (SOL) muscles. In brief, muscles was digested for 2 hours at 37°C in 0.2% (w/v) type I-collagenase (Sigma-Aldrich), reconstituted in DMEM (high-glucose, with L-glutamine, supplemented with 1% penicillin-streptomycin, GIBCO-Invitrogen). Following digestion, the muscle was transferred in plating medium (DMEM low-glucose, 10% HS, 1% penicillin-streptomycin, 0.5% chicken embryo extract, GIBCO-Invitrogen) and gently triturated with a wide bore pipette to release single myofibres. In each preparation, under phase contrast microscope, single fibers were carefully transferred in a 10 cm-plate containing 10 ml of muscle plating medium (1° dilution). Each single fiber

was subsequently transferred in another 10 cm plate containing 10 ml of muscle plating medium (2° dilution). Finally, each fiber was collected into one 50 ml Falcon tube with 1 ml of muscle proliferating medium (3° dilution in DMEM low-glucose, 20% FBS, 10% HS, 1% penicillin-streptomycin, GIBCO-Invitrogen, 0.5% chicken embryo extract, MP Biomedicals). Serial dilution was performed in order to avoid the presence of contaminant cells.

Cloning Satellite Cells from Single Myofibres

Clones of satellite cells were derived from EDL and SOL myofibres. After dilution, single fibers were triturated 20 times using a 18 G needle mounted onto a 1 ml syringe, to disengage SCs. The resulting cell suspension was diluted with proliferating medium and then dispensed into 96-well petri dishes with limiting dilution (0.5 cell/well). Dishes were incubated at 37.5°C, 5% CO_2 in a humidified tissue culture incubator.

Imaging Mitochondrial Membrane Potential

Tetramethyl rhodamine methyl ester (TMRM, 50 nM, Invitrogen) was used in "redistribution mode": the dye was allowed to equilibrate and was present continuously. The TMRM fluorescence intensity was quantified by removing background signals by "thresholding" and measuring the mean fluorescence of the pixels contained in mitochondria. Thus, the signal is independent of mitochondrial mass and only reflects the dye concentration within individual mitochondrial structures.

RT-PCR for Pfkfb3

Total RNA was isolated from HPC and LPC using Trizol (Invitrogen). Quantity and integrity of each samples was checked using Agilent BioAnalyzer 2100 (Agilent RNA 6000 nano kit). Three different aliquots of HPC and LPC RNA sample were retro-transcribed using GoScript™ Reverse Transcription System (Promega) following manufacturer instructions. Oligonucleotides used to amplify Pfkfb3 cDNA were previously described (Herrero-Mendez et al., 2009). Amplification was conducted using the following conditions: 4 minutes at 95°C; 95°C for 30

sec, 60°C for 30 sec, 72°C for 30 sec (35 cycles); final extension was carried out for 7 min at 72°C.

Immunofluorescence analysis

Immunofluorescence staining was conducted on HPC and LPC fixed in PFA 4%. Cells were permeabilized with 0.01% Triton X-100 in PBS for 1 min and blocked in BSA 1%, PBS pH7.5 for 60 minutes. Primary antibodies used were: mouse anti-ATPase b subunit (diluted in blocking solution 1:1000; Abcam, Cambridge UK) and goat anti-Pfkfb3 (1:100; Santa Cruz Biotechnology, Santa Cruz, CA. U.S.A. sc-10091). Secondary anti-mouse and anti-goat antibodies (1:500; Alexa Fluor, Molecular Probes, Invitrogen) were used. Nuclei were stained with 0.01% 4,6-diamino-2-phenylindole HCI (DAPI, Applichem) and the coverslips were mounted using Prolong Gold antifade reagent (Molecular Probes, Invitrogen). Negative controls were performed by omission of primary or secondary antibodies.

NADH Measurement

Mitochondrial "redox state" was measured from NADH auto-fluorescence using NaCN and FCCP to normalize the NADH signal to maximal reduction and oxidization.

Ca^{2+} analysis and C_2-Ceramide induced cell death

Coverslips were incubated with Fluo4 (10 μM) and Rhod-5N (10 μM) dyes to label the cytosolic Ca^{2+} and the mitochondrial network respectively. All fluorescent images were captured on Zeiss 510 LSM confocal microscope equipped with a 40X oil-immersion lens. For apoptosis treatment, cells were incubated for 8 and 10 hours with C_2-Ceramide (20 μM) to determine the number of living cells.

CO_2 measurement

Two different types of culture media were employed: DMEM which contains 4.5 mg/l (25mM) D-glucose, sodium pyruvate, $NaHCO_3$ 44 mM and DMEM with $NaHCO_3$ 44 mM and no glucose, supplemented with 25 mM of [U-^{13}C] D-glucose. Cells were cultured in optimal conditions in

hermetic screw caps 25 cm^2 flasks (Corning, Sigma Aldrich) at 1000 cells/cm^2. Media supplemented with [U-^{13}C] D-glucose was substituted to culture media and flasks were sealed for four hours. As control, cells were incubated in the same condition with DMEM high glucose (4.5 mg/l D-glucose). CO_2 production was determined on an isotope ratio-mass spectrometer after CO_2 extraction from culture media by means of acidification with glacial acetic acid. The ^{13}C to ^{12}C ratios of samples are expressed as differences from the international Pee Dee Belemate limestone (PDB) standard according to the formula $\Delta^{13}C‰ = [(^{13}C/^{12}C \text{ sample} - ^{13}C/^{12}C \text{ standard})/^{13}C/^{12}C \text{ standard}] \times 10^3$. The ratio of $^{13}CO_2$ over $^{12}CO_2$ produced is proportional to the quantity of oxidized glucose.

Statistical Analysis

Data are presented as mean ± s.d. Comparison between groups used the t-test assuming two-tailed distribution, with an alpha level of 0.05.

1.4.3 Results and Discussion

Muscle satellite cells were cultivated in matrigel-coated petri dishes avoiding cloning process. As first analysis, we established how to measure the level of CO_2 released in the medium as a new tool for the metabolic respiration (Figure 5a). To determine the level of carbon dioxide produced by SCs, we used D-glucose U-C_{13} 25 mM diluted in DMEM without piruvate and glucose. After 4 hours incubation, we analysed by mass-spectrophotometer the nmol of CO_2 released in the culture medium. In this study, we improved our investigation concerning SCs in terms of types of voluntary muscle fibers: slow twitch and fast twitch. Our previous research (Rossi et al., 2010) was focused only on SCs clone characterization without considering possible differences among muscles. For this reason, we chose EDL and *soleus* muscles as examples for fast-twitch and slow-twich muscle respectively. In figure 5a, we reported the nmol of CO_2 produced by treated and untreated cells. Our data revealed that in both muscles SCs increased the production of carbon dioxide compared to the untreated control cells. Treated cells derived from EDL muscle uncovered a statistical boost of CO_2

compared to SCs derived from *soleus* muscle (86.5 ± 16.3 versus 50.2 ± 11.0 respectively).

Likewise, SCs were cultivated for 24 hours in matrigel-coated petri dishes, and then loaded with TMRM for confocal microscopy. Rossi and colleagues previously demonstrated that assessment of the mitochondrial membrane potential ($\Delta\Psi_m$) with the potentiometric dye tetramethyl rhodamine methyl ester (TMRM) showed that HPC compared to LPC possessed an increased $\Delta\Psi_m$, reduced mitochondrial generation of ATP and higher rate of ROS production (Rossi et al., 2010). At resting conditions, abnormal rising of the $\Delta\Psi_m$ defined impairments in the H^+ transport through the Electron Respiratory Chain (ERC) as a result acting as a parameter to assess mitochondrial activity (Campanella et al., 2008 and 2009). Since this is normalized via pharmacological inhibition of the terminal enzyme of the ERC (the F_1F_o-ATPsynthase). In this case, we investigated the SCs membrane potential avoiding the cloning process. By this procedure, SCs highlighted two different subpopulations with a statistical difference in term of TMRM uptake: one with a low TMRM uptake (812 ± 398 arbitrary units, a.u.) and one with high TMRM uptake (2043 ± 362 a.u.; $p < 0.001$) (Figure 5b). More interestingly, this was in percentage equal to that of the clonal populations (LPC: 1121.68 ± 118.95; and HPC: 1595.52 ± 184.18 a.u., Rossi et al., 2010) thus indicating that differences in mitochondrial performance are present still at the very initial phases of the SCs' life and in this way account for inner heterogeneity before cloning and differentiation.

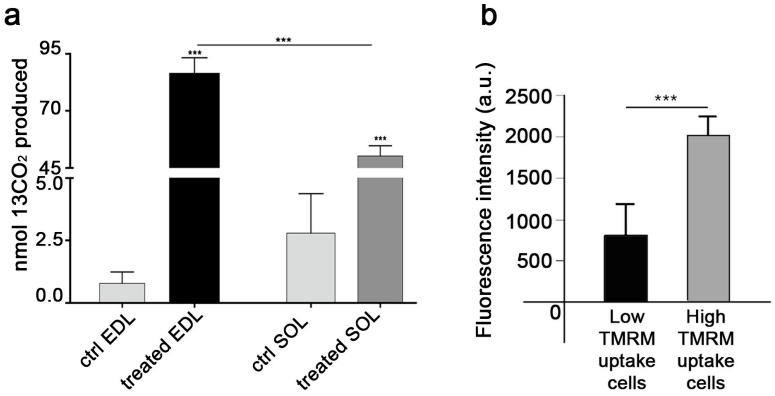

Figure 5: Different mitochondrial features in un-cloned satellite cells. (a) Measurement of CO_2 after incubation of D-glucose U-C_{13} for 4 hours, in un-cloned satellite cells derived from fast and slow-twitch muscle fibers. EDL SCs highlighted the higher level of CO_2 compared to *soleus* SCs ($p < 0.001$). (b) Time zero analysis: in 5 out of 5 preliminary experiments, after 24 hours of culture in muscle proliferating medium, SCs presented a different mitochondrial membrane potential $\Delta\Psi_m$ ($p < 0.001$).

Once established that cell physiology can underline differences within SCs population, even without cloning, we proceeded on SCs clones' characterization. Our aim was to further understand the differences between LPC and HPC, not only in terms of differentiation pathways but also in their signalling mechanism that could explain the inner metabolic marks.

The "redox state" is related to the Reactive Oxygen Species (ROS) (Aguiari et al., 2008; Pelicano et al., 2008) and we already estimated the level of ROS in both clones (Rossi et al., 2010). For this reason, we examined reduction-oxidation potential via measurement of the mitochondrial NaDH (Nicotinamide Adenine Dinucleotide H). This kind of metabolic inspection does not require any exogenous dye since based on the auto-fluorescence of the mitochondrial pyridines via a dedicated UV laser. The outcome of this analysis is reported in the following figure, and clearly showed the alternative state of mitochondrial oxidation. The normalized values reflected the state of resting respiration and originated from a standard experimental maneuver (Campanella et al., 2008), in which the cells undergo pharmacological treatment with mitotoxins. This process induced maximal reduction (by inhibiting the respiration with NaCN), and maximal oxidation (triggered with the un-coupler FCCP) to set the extremes of the respiratory performance extrapolating the starting levels. This -as indicated in the plotted data- proved LPC and HPC to be opposite for their "Redox State" with LPC more oxidative -hence mitochondria more coupled- and the HPC much more reduced, implying mitochondria less coupled (Figure 6a). The NAD^+/NADH evaluation confirms the previous records and emphasizes that HPC do have a greater glycolytic metabolism compared to LPC (824.9 ± 104.9 and 1121.3 ± 141.7 a.u. respectively) ($p < 0.05$).

To corroborate further this data, we used the same protocol of un-cloned SCs to measure the CO_2 production. In figure 6b, we reported the nmol of CO_2 produced by treated and untreated cells. In both slow and fast-twitch derived cells, all treated clones released a higher amount of CO_2 compared to the control ($p < 0.001$). However, only LPC highlighted a statistical increased CO_2 level in the fast-twitch muscle. In any case, HPC produced a higher level of CO_2 (76.7 ± 1.8 and 66.3 ± 15.1 for EDL and *soleus* respectively) compared to LPC (61.3 ± 3.9 and 35.0 ± 3.5 for EDL and

soleus respectively) in both muscle types confirming that the high proliferative clones possess a glycolytic metabolism (Figure 6b). Thus sustaining the theory by which HPC are more inclined to glycolytic respiration consequent depression of the mitochondrial oxidation.

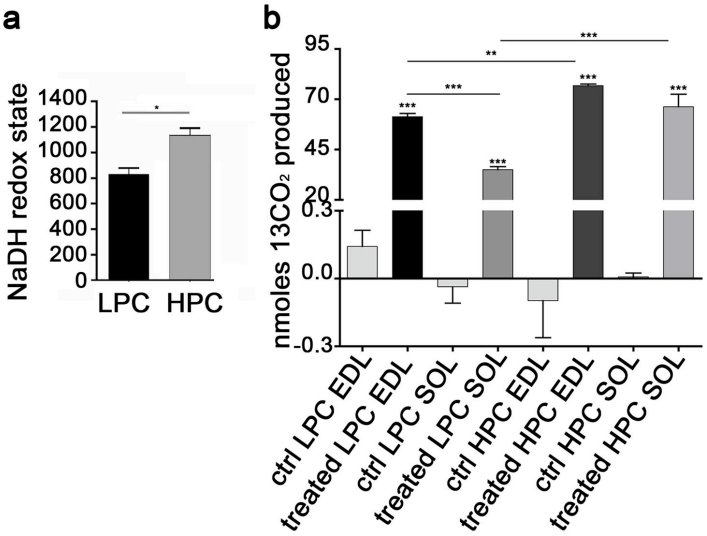

Figure 6: Metabolic study of satellite cell clones. (a) Measurement of NaDH level: HPC and LPC demonstrated different redox states. These data confirmed that HPC has a glycolytic metabolism compared to low proliferative clones ($p < 0.05$). (b) Measurement of CO_2 after incubation of D-glucose U-C_{13} for 4 hours, in SC clones derived from fast and slow-twitch muscle fibers. Treated cells produced a higher amount of CO_2 compared to untreated control cells ($p < 0.001$). However, only LPC from fast-twitch muscle had a significant increased level of CO_2 compared to the slow-twitch muscle ($p < 0.001$).

However this needed to be confirmed by evaluating of the enzymatic pathways that frame cell metabolism and the expression of the glycolytic enzyme Pfkfb3 (6-phosphofructo-2-kinase/fructose-2,6-biphosphatase 3) was checked with this finality. The energy and anabolic substrates during the cell cycle must be efficient and tightly coupled to the regulation of metabolism and growth.

Fructose 2,6-bisphosphate (Fru-2,6-BP) is an activator of 6-phosphofructo-1-kinase (PFK-1), an enzyme that is essential in glycolysis. Throughout the last thirty years, it is now established that Pfkfb3 (6-phosphofructo-2-kinase/fructose-2,6-biphosphatase 3) has a particular interest because it is activated in human cancers and increased by mitogens and low oxygen (Herrero-Mendez et al., 2009; Yalcin et al., 2009). To run this assay, we retro-transcribed RNA from both clones and using RT-PCR we were able to recognized that Pfkfb3 mRNA is more expressed in HPC, but still slightly

present in LPC (Figure 7a). Hence, the agarose gel signal demonstrated that HPC possessed a statistical higher expression in comparison to LPC (Figure 7b). Our data was confirmed statistically ($p < 0.05$), and the translation into protein was also investigated via immunofluorescence. This analysis also established the same proportions of enzyme's expression indicated by the RT-PCR assay with a greater quantity in HPC than in LPC (Figure 7c – e). The relative quantification is reported in figure 7e confirmed that, although both clonal types are efficient for this enzymatic pathway, HPC do possess it in larger quantity. Through protein array analyses, Yalcin and colleagues found that the expression of cell cycle proteins, such as cyclin-dependent kinase (Cdk)-1 was increasing in presence of Pfkfb3, while its universal inhibitor p27 was decreasing (Yalcin et al., 2009). These observations revealed that Fru-2,6-BP might couple the activation of glucose metabolism with cell proliferation. Taken together, all these remarks could explain the differences between HPC and LPC in terms of proliferation and differentiation processes.

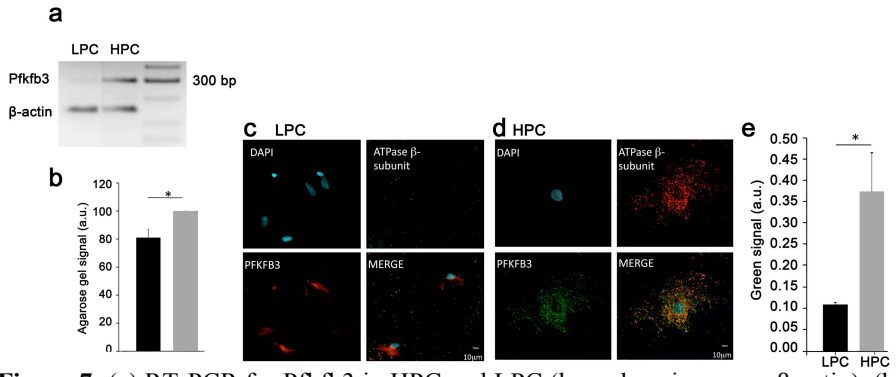

Figure 7: (a) RT-PCR for Pfkfb3 in HPC and LPC (housekeeping gene: β-actin). (b) Agarose gel signal between HPC and LPC ($p < 0.05$). (c) Immunofluorescence for ATPase β-subunit and Pfkfb3 in LPC and (d) HPC (bar: 10 µm). (e) Intensity of Pfkb3 signal ($p < 0.05$).

An inter-organelle communication has emerged throughout the study of mitochondrial Ca^{2+} signalling (Szabadkai et al., 2008). In fact, mitochondrion controls not only their own Ca^{2+} concentration, but it also influences the entire cellular network, including the endoplasmic reticulum, the plasma membrane, and the nucleus. In particular, Ca^{2+} homeostasis and signalling regulate several cellular functions of the whole cell providing a framework by which mitochondrial biogenesis, shape, and metabolic performance will adapt during proliferation and cellular stress. Therefore, we examined the basal physiology belonging to HPC and LPC investigating

the mitochondrial uptake of Ca^{2+}. HPC and LPC were loaded with rhodamine-5N (McNamara et al., 2005; Sobinet et al., 2008) to label the mitochondrial network to be able to follow the uptake of Ca^{2+} from the endoplasmic reticulum into the mitochondrion. Through the confocal microscopy, the mitochondrial Ca^{2+} uptake was tracked after cells challenge with the IP_3 generating stimulus ATP 1mM (Figure 8a). The maximum uptake level of Ca^{2+} was recorded and calculated as means of the peaks' values (Figure 8b) with the following result: higher mitochondrial Ca^{2+} uptake in LPC than in HPC (3.3 ± 0.7 and 1.6 ± 0.5 normalized value respectively), suggesting a possible correlation with apoptosis susceptibility.

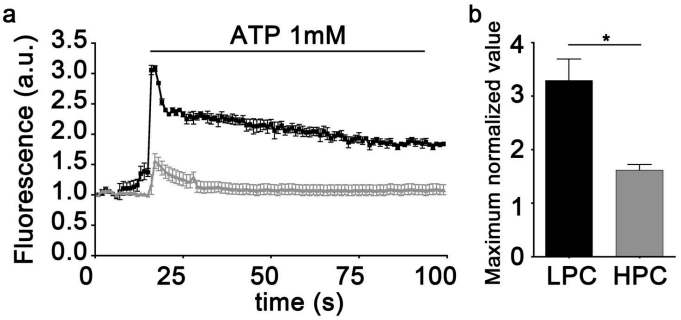

Figure 8: (a) Mitochondrial calcium level was followed in real time by measuring Rhod-5N dye. LPC and HPC were treated with ATP 1 mM and traces trend monitored over time. (b) The diagram explained the maximum uptake of calcium in both clones ($p < 0.05$).

Since Ca^{2+} mediates apoptosis (Campanella et al., 2004), we then exploited whether LPC are more permissive to apoptosis. Hence, we treated our clones with C_2-Ceramide 20 μM for 8 and 10 hours (Figure 9a – b). Cell counting was normalized by the total number of cells for each type of clone in both conditions. After 8 hours, HPC highlighted substantial resistance to cell death as no differences between untreated and treated cells were found (248.8 ± 61.0 versus 264.0 ± 54.4 respectively), while LPC showed significant sensitivity to death compared to the untreated control of the same cell type (126.6 ± 12.3 versus 244.4 ± 49.5 respectively) ($p < 0.001$). However, the comparison between HPC and LPC treated cells highlighted a statistical significance of alive cells in HPC ($p < 0.01$) (Figure 9a).

The same results were obtained after 10 hours incubation, emphasizing that the highest amount of alive cells were found in HPC compared to LPC (194.8 ± 16.2 versus 59.2 ± 30.8 respectively) ($p < 0.001$) (Figure 9b).

These data confirmed our assumption that HPC is less permissive to apoptotic stimuli because of the less intake level of Ca^{2+}.

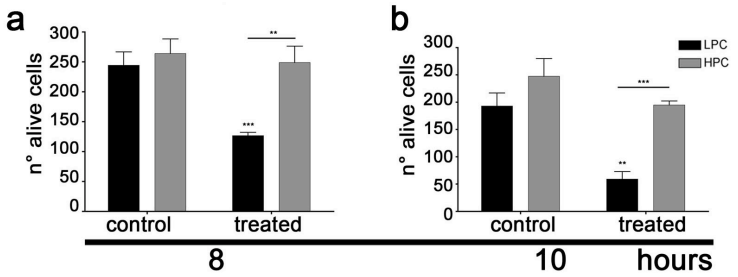

Figure 9: (a – b) C_2-Ceramide (N-Acetylsphingosine) treatment after 8 and 10 hours respectively: the charts highlighted the number of alive cells after incubation with ceramide 20 µM between control (untreated) and treated clones. After 10 hours of incubation C_2-Ceramide HPC showed an increased rate of alive cells compared to LPC, meaning that the high proliferation rate has influenced the apoptosis induction ($p < 0.01$ and 0.001).

Once ascertained that HPC has different metabolic features compared to LPC, we explored the potential variations among mitochondria volume fraction within the SCs clones. To do so, we loaded our cells with Fluo4 and rhodamine-5N to label the cytosolic Ca^{2+} and the mitochondrial network respectively. The ratio between the two signals was measured, and as consequence we proved evidence of an increased mass into LPC (2.5 ± 0.7 and 0.80 ± 0.1 respectively) (Figure 10a). This is in line with a greater mitochondrial activity of HPC.

The resistance to intrinsic apoptosis is a consequence of a reduced efficiency in the mitochondrial Ca^{2+} handling, and denotes a phenotypic cellular physiology that is logically associated with an ability to proliferate more robustly -as it is for every cell type with marked glycolytic profile. The greater sensitivity to apoptosis of the LPC likewise the greater buffering capacity for Ca^{2+} sustain a metabolically active condition that is indispensable for a myogenic fate as shown in precedence (Rossi et al., 2010). If this were true, HPC would instead preserve a stem-like potential till the lineage commitment. To validate this, each clone used for the above experiments was sub-cloned and analyzed after 10 days in culture and, as reported in figure 10b. LPC gave rise exclusively to LPC sub-clones, whilst HPC showed the presence of both subpopulations in a ratio similar to what we already published (Rossi et al., 2010) (85.9 ± 5.5% and 14.1 ± 5.5% versus 75% and 25%) (Figure 10b).

This added evidence sustains our initial hypothesis and emphasizes that the inner heterogeneity between SCs embeds a different predisposition to myogenic lineage demonstrating that the stemness lies exclusively into HPC instead of the already committed LPC.

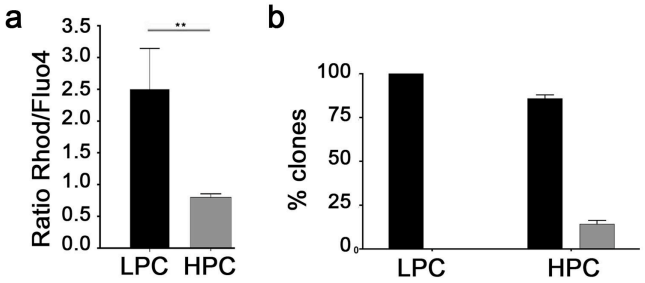

Figure 10: (a) Mitochondrial mass analysis showed statistical difference between HPC and LPC in term of the size of mitochondrial network ($p < 0.01$). (b) Sub-cloning of HPC and LPC demonstrating that only HPC could give again both clones.

Taken together, all these data reveal that we identified the carbon dioxide measurement as a promising tool able to distinguish differences between SCs clones derived from fast and slow-twitch muscles. Besides that, some of these metabolic assays were useful to identify the intrinsic heterogeneity of the satellite cells, even without the cloning process. In addition, our records indicated that SC clones possess a distinct and precise metabolism. In particular, HPC and LPC could be distinguishing by mitochondrial analysis demonstrating that cell physiology could be a useful test and a good marker in terms of cell characterization. Lastly, HPC proved to be more glycolytic confirming what we already published, and it also may represent the stem cell within the SCs clonal population.

Chapter II

2. Introduction

The part of the peripheral nervous system (PNS) that controls both the peristaltic and secretory activity of the gut wall is the enteric nervous system (ENS). It is composed of a large number of neurons and glia, which are organised into interconnected ganglia distributed throughout the length of the gut (Gershon et al., 1994; Le Douarin, 1999).

During embryogenesis, the vagal neural crest generated the majority of neurons and glia of the ENS (Le Douarin et al., 1973; Yntema et al., 1954). These cells, knows as neural crest cells (NCCs), moved through the foregut mesenchyme colonising the entire length of the gut over a period of 4 days (Durbec et al., 1996). However, the result of a failure of complete colonisation of the gut by NCCs is the absence of enteric ganglia (aganglionosis), usually in the colon, leading to peristaltic misregulation and severe intestinal obstruction: Hirschsprung's disease. This syndrome represents the main genetic cause of functional intestinal obstruction with an incidence of 1:5000 live births. It is congenital malformation of the hindgut characterised by the absence of parasympathetic intrinsic ganglion cells in the submucosal and myenteric plexuses. The proto-oncogene RET (REarranged during Transfection), mapping in 10q11.2, is the major gene predisposing to the disease (Amiel et al., 2008).

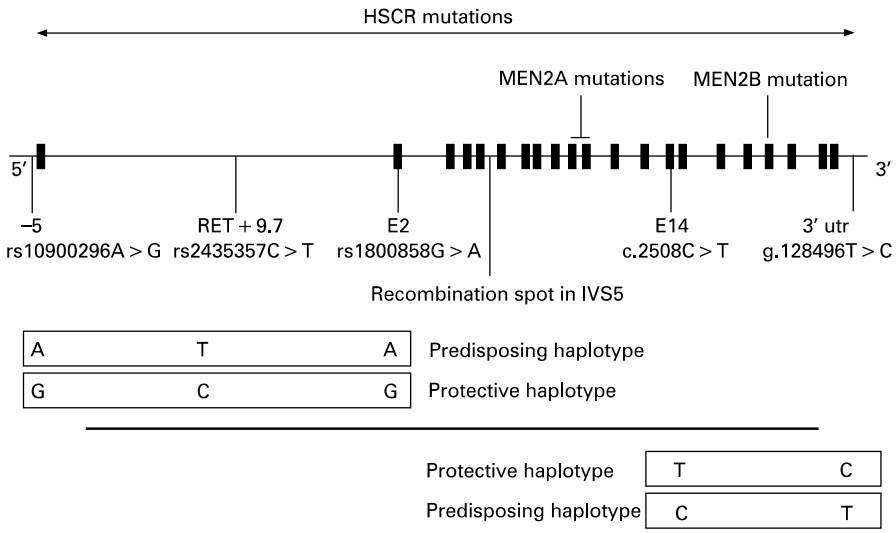

Figure 11: Mutations, haplotypes and recombination spot at the RET locus (from Amiel et al., 2008).

2.1 Neural crest cells

NCCs are a transient population of multipotent cells that arise following

closure of the neural tube. They migrate extensively throughout the embryo and give rise to a wide variety of cell types including melanocytes, the skeletal and connective tissues of the face, neurons and glia of the sensory, sympathetic, and the ENS (Le Douarin et al., 1973).

During embryogenesis, the lung buds arise by a process of evagination from a presumptive respiratory territory in the ventral wall of the primitive foregut. After initial bifurcation, the entire bronchial tree and associated lung lobes are formed during a prolific branching period (Chinoy MR, 2003). From early in development, the lung buds become invested with mesenchyme-derived airway smooth muscle (ASM) that encircles the epithelial buds and the bronchial tree. ASM rapidly becomes functionally active, exhibiting phasic contractions that persist throughout the prenatal period (Schittny et al., 2000). The development of networks of neural tissue in the form of ganglia and nerve processes is closely associated with the formation of ASM around the growing airways. Although neural development in the lung has been documented in a range of species including mouse (Tollet et al., 2001), pig (Weichselbaum et al., 1999), and human (Sparrow et al., 1999).

Since the lung bud primordia undergo evagination and begin branching concomitant with the migration of NCCs along the foregut to form the ENS of the gastrointestinal tract, it was postulated that some of these NCCs may also colonize the lung and subsequently form neurons (Dey et al., 1997). Burns and colleagues confirmed this hypothesis using quail-chick inter-species grafting to fate map NCCs. Their results showed that neural tissue within the lung originates from vagal NCCs, and these very cells migrate from the foregut into the developing lung buds to differentiate into neurons and glia (Burns et al., 2005 and 2008). Recently, they also established that the embryonic and foetal human lung ganglia are neural crest-derived (Burns et al. 2008), as neural tissue that develops around the bronchi and epithelial tubules in close association with airway smooth muscle co-localizes with $p75^{NTR}$, a specific marker for migrating NCCs (Barlow et al., 2008).

2.2 RET gene and Hirschsprung's disease

RET signalling is already known to be necessary for the migration of NCCs within the gut; its lost results in gut aganglionosis in mice (Schuchardt et al., 1994), and it is the main gene implicated in the congenital aganglionic gut disorder, the Hirschsprung's disease in humans (Amiel et al., 2008). Young and colleagues already demonstrated that NCCs expressed the RET receptor and GFRα1 co-receptor, while the ligand GDNF (Glial-cell-line-Derived Neurotrophic Factor) has been shown to be a chemo-attractant for NCCs (Young et al., 2001). Taken together, these studies entailed that RET signalling could be of critical importance for the normal development of lung innervation.

For this reason, Freem and colleagues showed that labelled NCCs (YFP-positive) start to migrate into the lung from the oesophagus region at embryonic day E10.5 to form an extensive branching network in association with the developing airways. They also proved that YFP cells are able to respond in a chemo-attractive to GDNF suggesting the involvement of the RET signalling pathway during lung development. In spite of this, they did not detect any apparent differences in the extent of lung innervation of $Ret^{-/-}$ and $Gfr\alpha1^{-/-}$ embryos. This implied that the role of the RET signalling in the development of the lung innervation requires further investigation (Freem et al., 2010).

2.3 Neural crest cells and smooth muscle differentiation

The variable distribution of migrating vagal NCCs within the gut may be partly dependent on the smooth muscle (SM) differentiation. At the early stages of development, NCCs were distributed within the splanchnopleural mesenchyme. As soon as the circular muscle began to differentiate, vagal cells were distributed on either side of the denser muscle layers. Consequently, in order to colonise the ENS, vagal NCCs may take the path of least resistance within gut regions high in molecules, which are known to play an important role in NCCs migration. Nonetheless, the situation is likely to be more complex.

Recently, the role of NCCs in mammalian vascular development was examined with a genetic approach (Wnt1-Cre mice crossed with a floxed

stop Rosa26 reporter mice). The resulting activation of a lacZ reporter gene in NCCs served as a sensitive lineage marker. This analysis showed that NCCs contributes SMCs to the ascending and arch portions of the aorta, the arterious ducts, the right subclavian arteries, and the right and left common carotid arteries. At the same time, these data showed that SMCs are not derived from NCCs in the descending thoracic aorta, abdominal aorta, coronary arteries, pulmonary arteries, left subclavian artery, and distal portions of the internal carotid arteries because cells were not labelled by the Wnt1-Cre lineage marker (Jiang et al., 2000). These results were then repeated by another group using different genetic lines (Nakamura et al., 2006). As in chick-quail chimeras, NCCs lineage markers did not label endothelial cells, and the adventitia also appeared to derive from an origin other than neural crest (Majesky MW, 2007).

2.3.1 Smooth muscle stem cells in embryos

The most well characterized population of smooth muscle stem cells in the embryo is found in the cranial neural crest. NCCs form at the mediolateral border between the neural plate and the epidermis in response to graded bone morphogenetic protein (BMP) signalling (Sasai et al., 1997). These cells give rise to multiple cell types at different axial levels, including: sympathetic and sensory nerves; glial cells; melanocytes; cartilage; bone; fibroblasts and smooth muscle cells (SMCs).

The cranial neural crest, which is located anterior to somite 5, generates migrating multipotential progenitor cells. In 1975, LeLievre and colleague reported the first detailed fate maps that revealed a neural crest origin for vascular SMCs. In these pioneering studies, a segment of cranial neural tube from an early quail embryo was grafted into an equivalent position of a developmental stage-matched chick embryo. As result, the majority of cranial neural crest cells migrated into the pharyngeal arch complex, became closely associated with endothelial cells of the branchial arch arteries (BAAs), and differentiated into vascular SMCs (LeLievre et al., 1975) (Figure 12).

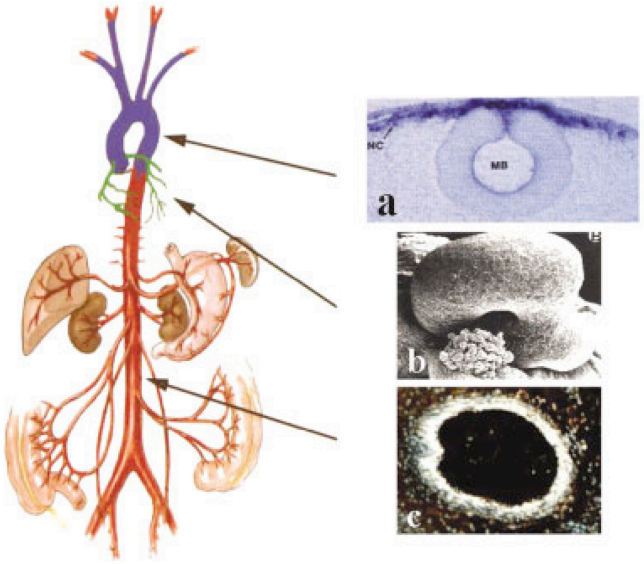

Figure 12: Fate mapping studies in chick and mouse embryos have identified at least three independent origins for vascular SMCs in the embryo. **a:** Vessels in blue recruit SMCs from progenitors that originate from cardiac neural crest stem cells. **b:** Coronary SMCs (green) arise from mesothelial progenitor cells that line villus-like projections of the proepicardial organ (PEO). **c:** Vessels in red recruit SMCs from either lateral or splanchnic mesoderm depending on their location within the embryo (from Hirschi et al., 2004).

Migrating NCCs also contributed to neuronal and connective tissue cells in the adventitial layer of these vessels. In late 80s, two different groups discovered that segments of either trunk or mesencephalic neural crest were unable to rescue the lethal developmental defects resulting from deletion of the cranial neural crest (Bockman et al., 1987; Kirby M., 1989). These results suggested that ectomesenchymal cells in the cranial neural folds are competent to form SMCs, and that NCCs cannot be reprogrammed by environmental signals, at other axial levels.

2.3.2 Differentiation vs self-renewal

NCCs can differentiate into various cell types while undergoing self-renewal, a property characteristic of stem cell populations. Different cell fates are thought to result from progressive restrictions in lineage potential. Two models were proposed:

1. An instructive differentiation occurs when multipotential cells respond to signals in the local environment that directs them to one cell fate or another.

2. NCC can undergo stochastic commitment to specific cell fates followed by selection and amplification of survivors governed by apoptotic and survival signals in the local environment.

However, the actual process probably lies somewhere in between, in which cell-intrinsic determinants interact with environmental signals to produce the right cell types in the right place and time during development (Hirschi et al., 2004).

2.3.3 Cell fate determinants

As discussed above, combinations of determinants mediate NCCs fate decisions. Genetic analysis has identified some of these factors that play key roles in their lineage commitment and differentiation (Table 1).

Intrinsic determinats	Function	Extrinsic determinats	Function
Pax3	Transcriptor factor	Endothelin	Growth/survival factor
Fox C1/C2		Retinoic acid	Morphogen
Tbox1		Wnt/Frizzled	Growth/survival factor
Cx43	Gap junction protein	FGF8	
PDGF-Rα	Growth factor receptor	BMP2	
PitX2	Transcriptor factor		

Table 1: Fate determinants of cranial neural crest stem cells.

Pax3/splotch

Discussed in chapter one.

Forkhead-winged helix genes (FoxC2, FoxC1)

Yamagishi and colleagues identified an upstream element in the Tbx1 locus that binds FoxA2, FoxC1, and FoxC2, and mediates transcriptional activation of Tbx1 by these Fox family. These studies identified a hedgehog-responsive target gene that controls NCCs fate in the pharyngeal arch complex members (Yamagishi et al., 2003).

Tbox 1

Tbx1 is a member of the Tbox family of binding domain transcription factors. Its deletion causes the DiGeorge syndrome (DGS), one of the most common genetic disorders that results in numerous physical manifestations including craniofacial, glandular and cardiac anomalies. Deletion of one copy of Tbx1 disrupts development of the fourth pharyngeal arch artery,

whereas the homologous knockout produces severe defects throughout the pharyngeal arch complex (Lindsay et al., 2001). Vitelli and colleagues reported that Tbx1 deficiency causes distinct vascular and heart defects, suggesting multiple roles in cardiovascular development (Vitelli et al., 2002a). Tbx1 and Fgf8 exhibit genetic interactions in development of the aortic arch arteries and Fgf8 appears to be a critical signal that directs NCCs migration and/or survival during aortic arch artery formation (Hirschi et al., 2004).

Connexin 43 (Cx43)

Cx43 gap junctions contain adherents' junctions that are found in migrating cardiac NCCs. Loss of function of either gene product results in altered crest cell motility and reduced cell survival. On the contrary, increasing expression results in increased numbers of cardiac neural crest cells detected in the outflow septum of the developing heart (Huang et al., 1998). Changes in cardiac myocytes proliferation correlate closely with an increase or decrease in NCCs numbers in the cardiac outflow tract of mice with different levels of Cx43 expression (Hirschi et al., 2004).

PDGF-receptor α

Conditional deletion of a floxed PDGF-Rα allele in NCCs upon crossing with Wnt1-Cre mice showed a specific requirement for PDGF-Rα in cranial mesenchyme and for proper formation of aortic arch arteries (Tallquist et al., 2003). The most prevalent defect in PDGF-Rα conditional knockout embryos is the anomalous origin of the right subclavian artery from the pulmonary trunk. However, the underlying mechanisms involved remain unclear. On the other hand, no differences were found in cell proliferation, migration, and survival or SMCs differentiation between wild type and knockout PDGF-Rα NCCs (Tallquist et al., 2003).

Pitx2

Pitx2 is a paired-related homeobox gene that plays important roles in establishment of left-right asymmetry, formation of the cardiac outflow tract, and remodelling of aortic arch arteries.

Endothelins (ETs)

ETs 1, 2 and 3 are a family of small peptides (21 amino-acids) that play important roles in NCCs differentiation and survival (Yanagisawa et al., 1998). ETs 1-3 activate G protein-coupled ET receptors endothelin receptor (EDNR). $ET1^{-/-}$ embryos exhibit hypoplasia of aortic arch arteries, aberrant right subclavian artery, and an incompletely interruption of the aortic arch (Kurihara et al., 1995).

Retinoic acid (RA)

In vitro studies have shown that RA acts upon NCCs to promote differentiation to neuronal lineages. Its rate-limiting step is the activity of retinaldehyde dehydrogenase (Raldh). Raldh-2 is the major form of the enzyme found in embryonic tissues and knockout mice are embryonic lethal by E10.5 and exhibit a complex variety of cardiac defects (Niederreither et al., 2001).

FGF8

The expression pattern of FGF8 is similar to those of Tbx1 in the developing pharyngeal arch complex, and is candidate paracrine mediator, while its mRNA is strongly down regulated in $Tbx1^{-/-}$ embryos (Vitelli et al., 2002b). Previous studies had shown that severe reductions in FGF8 expression caused increases in neural crest cell death (Abu-Issa et al., 2002).

Bone morphogenetic protein-2 (BMP2)

BMP2 is expressed in the dorsal aorta and is involved in the production of sympathetic neurons by NCCs emanating from the trunk level. BMP2 induces the expression of MASH1, a bHLH factor required for sympathetic neuron formation.

In vitro enhancement of muscle precursor cells differentiation by co-cultures with neurogenic stem cells

2.4.1 Background

The majority of the enteric nervous system (ENS) is derived from vagal neural crest cells (NCCs), and these progenitors have been postulated to be an appropriate source of cells for the treatment of Hirschsprung's disease (HSCR; congenital megacolon).

HSCR is the most common form of congenital intestinal obstruction (1:4500 live births), which results from failure of enteric ganglia to develop in the distal bowel (colonic aganglionosis). The familial form of HSCR has been associated mainly with mutations in RET, a locus encoding a tyrosine kinase receptor for members of the GDNF family of ligands (Amiel et al., 2008).

Cultures of NCCs progenitors isolated from avian and mammalian embryos have served as valuable *in vitro* systems to study the role of extracellular signals and intracellular transcription factors in cell commitment and differentiation in the peripheral nervous system (PNS) (Bondurand et al., 2006). Above-mentioned progenitors have also been isolated from the gut of rat and mouse embryos. In addition, neurospheres generated from both mouse and human tissues contain proliferating neural crest-derived cells that could be expanded in tissue culture to generate both glial cells and neurons. These cells are also obtainable from murine and human postnatal gut by representing for future clinical applications an easily suitable neuronal cell source.

On the other hand, MPCs are a pool of satellite cells in proliferation, and represent a very homogenous population concerning the original sublaminal localization and marker expressed. Nonetheless, as we already discussed in chapter one, MPCs show the presence of different subpopulations with a really heterogeneous behaviour when they are cultured *in vitro* or *in vivo*.

This study was done in collaboration with N. Thapar's group, which is responsible for neurosphere-like bodies (NLBs) generated from enteric precursor cells (Bondurand et al., 2006). Our purpose was to determine how NBLs -from the enteric nervous system- in presence of MPCs could enhance skeletal and smooth muscle cells differentiation. To do so, MPCs and NLBs were co-cultured for 2 weeks in myogenic medium. As first step, different ratios were used to identify the best condition that enhances

myoblasts fusion. Secondly, western blotting and immunofluorescence analysis were performed to determine the proper level of both myogenic and neural proteins expression.

Smooth muscle (SM) is a morphologically distinct tissue that mediates the contraction of hollow organs in the circulatory, respiratory, gastrointestinal and urogenital systems. It is also present in a variety of anatomical locations, such as the hair follicles, irises, and lachrymal ducts.

SMCs are the main cell type in SM tissue and their sarcomeres are arranged with no specific banding pattern. These cells share many lineage-specific markers, such as smooth muscle α-actin (αSMA), myosin heavy chain, SM22α, calponin and caldesmon (Owens et al., 1997). Owens and colleagues reported that common cis-acting elements in the promoter regions of SM lineage markers provided new insights into how SMCs differentiation is initiated and maintained (Owens et al., 2004). Many SMC-specific genes promoters contain CArG [CC(A/T)6GG] boxes or CArG box-like sequences and their expression is triggered by cooperative binding of the ubiquitous serum responsive factor (SRF) and the SMC-specific co-activator myocardin to CArG sequences (Wang et al., 2001; Owens et al., 2004). Also unclear are the temporal and spatial patterns in which these transcription factors act to initiate or maintain SMCs differentiation programs (Chi et al., 2007).

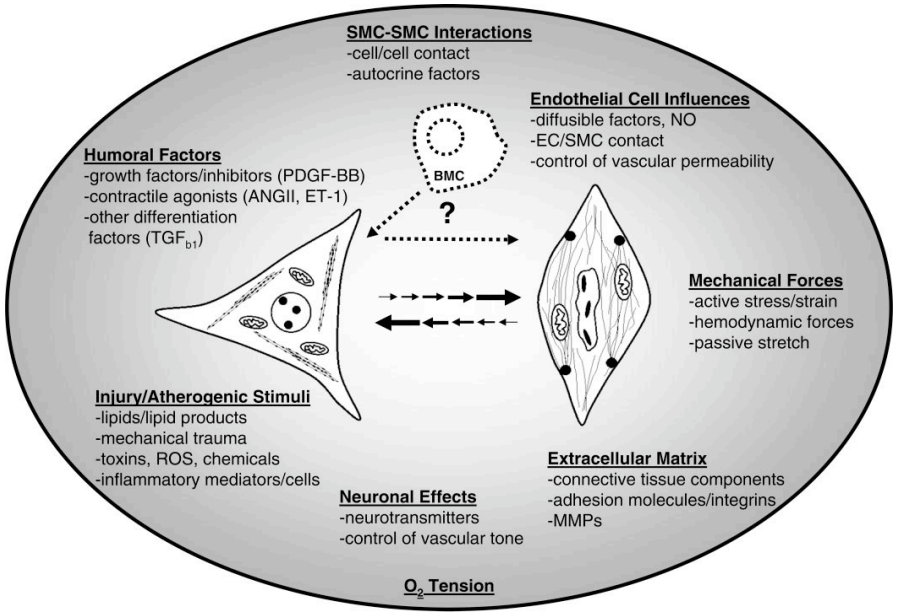

Figure 13: This cartoon summarizes some of the extrinsic factors or local environmental cues that are either known or believed to be important in influencing their differentiation/maturation state. The multiple arrows connecting the cell types are meant to illustrate the complexity of steps involved in transitions between the different phenotypes and the fact that changes appear to be reversible. Two separate pathways are depicted rather than a single reversible pathway, since it is not at all clear that transitions in phenotype follow the same pathway. Furthermore, there is considerable controversy as to the relative contribution of bone marrow-derived progenitor cells (BMC) in the developing neointima and whether these cells are capable of becoming fully differentiated SMCs (as indicated by the "?" and the dashed arrows). PDGF, platelet-derived growth factor; ET, endothelin; TGF, transforming growth factor; ROS, reactive oxygen species; NO, nitric oxide; EC, endothelial cells (from Owens et al., 2004).

Even if SMCs share many morphological and molecular features, they carried out distinct functions in different organs and tissues and diverged significantly in their contractile and mechanical properties, hormonal control, physiological regulation, and pathological alterations (Majesky MW, 2007).

Unlike skeletal and cardiac muscle cells, which are terminally differentiated, mature SMCs retain their ability to undergo large-scale, reversible phenotypic modulations in response to various genetic and environmental influences (Halayko et al., 2001; Chen et al., 2006). This phenotypic plasticity plays an important role in the pathogenesis of human diseases. SMCs are commonly found in cancers as components of blood vessel walls having abnormal morphology and sometimes fail to express the appropriate SM differentiation marker genes (Morikawa et al., 2002). These structural abnormalities contribute to the spatial and temporal heterogeneity in tumour blood flow, as result the tumour micro-environments play a major role in cancer progression and treatment failure (Jain RK, 2005).

2.4.2 Materials and Methods

Animals

Four-month-old wild-type mice [strain C57BL/6J; Jackson Laboratories, Bar Harbor, ME, USA] mice were used to collect myofibres and culture satellite cells. Wild-type whole foetal gut and postnatal gut peels were isolated from Parkes (outbred) mice. Mutant guts were isolated from GFP-ve mice. The day of vaginal plug detection was considered to be E0.5.

Satellite cells isolation and culture

Flexor digitorum brevis (FDB) muscles of the hind feet are carefully removed (tendon-to-tendon) and single fibers obtained by enzymatic dissociation with collagenasi are plated onto Matrigel™ (BD Bioscences) coated dishes and left undisturbed for five days. After this time, the satellite cells that have migrated off onto the plate have reached 70-80% confluence and are trypsinized and kept in culture for 2-3 more passages in proliferating medium (DMEM low glucose, 20% of foetal bovine serum, 10% of horse serum, 0.5% of chicken embryo extract and 1% penicillin-streptomycin).

Dissociated gut cultures and generation of NLBs

To generate neurosphere-like bodies (NLBs) from foetal gut tissue, whole gut was dissected from E11.5 embryos in L15 medium (Invitrogen, UK), washed with Ca^{2+}- and Mg^{2+}-free PBS (Invitrogen, UK) and digested for 6 minutes with a mixture of 1 mg/ml dispase/collagenase (Roche, UK) at room temperature (RT). Dissociated tissue was washed sequentially with PBS and NCCs culture medium, which included 15% chicken embryo extract and basic fibroblast growth factor (bFGF; 20 ng/ml; R&D Systems), and plated onto tissue culture dishes coated with 20 μg/ml fibronectin (Sigma). Cultures were re-fed every 2 days. Once NLBs appeared, human recombinant epidermal growth factor (hrEGF) (20 ng/ml; Calbiochem) was added to the medium. To isolate NLBs were trypsinised at RT, washed with NCSC medium and passed through a mesh (pore size 50 μm) to produce a near single cell suspension, which was plated as before. Cells were infected using a mixture of NCCs medium and a GFP-expressing retrovirus suspension (1:1) in the presence of polybrene (5 μg/ml). GFP-expressing cells were isolated 24 hours later by fluorescence activated cell sorting (FACS) and plated in complete NCCs medium at a density of 50-100 cells per Sonicseal™ well and cultured for up to 15 days. Human recombinant (hr) GDNF protein (Peprotech) was used at 10 ng/ml either in complete medium or in NCCs medium lacking CEE, EGF or FGF.

Immunofluorescence analysis

Immunofluorescence analysis was conducted after 14 days of co-culture. MPCs and NBLs were fixed with 4% paraformaldehyde (PFA; Sigma-

Aldrich) in phosphate buffered saline (PBS, GIBCO-Invitrogen), rinsed in PBS and permeabilized with Triton X-100 (Fluka) 0.5% in PBS. After washing, cells were incubated with primary antibodies overnight at 4°C or 1 hour at 37°C. Non specific interactions were blocked with 20% goat serum (Vector). They were then washed and incubated with labelled secondary antibodies for one hour at room temperature. Cells were then mounted with fluorescent mounting medium (DAKO) plus DAPI 100 ng/ml (Sigma-Aldrich).

The primary antibody was used rabbit anti-mouse Troponin I (Abcam, dilution 1:100). Secondary antibody used was Alexa Fluor chicken anti-rabbit 594 (Molecular Probes).

Western blotting

Cells were washed into 10 mM Tris base buffer, pH 7.3, containing 3 mM NaCl, 100 mM KCl, 3.5 mM MgCl2 and 6% sucrose. They were broken by sonication for 3 x 5 seconds (MSE Sonyprep; MSE, Crawley, Surrey, UK) in the presence of protease inhibitors, and the protein concentrations of each sample determined with a Bio-Rad Protein Assay (Bio-Rad, München, Germany). Samples were loaded onto SDS-PAGE gels and after electrophoresis transferred to nitrocellulose. After blocking, blots were probed with primary antibody. The blots were then washed and incubated with horseradish peroxidase-conjugated secondary antibodies according to the manufacturer's instructions (Amersham Biosciences, Piscataway, NJ). The enhanced chemiluminescence (CL) system and exposure to film was used to visualize the bands, taking a number of different exposures.

2.4.3 Results and Discussion

Satellite cells were obtained by culturing into matrigel-coated petri dishes single mouse fibers after their isolation (Figure 14a-c). Just after 48 hours, SCs are coming out from the parental myofiber (Figure 14b), and in less than one week their number increase exponentially (Figure 14c).

As a first step towards establishing a cell culture protocol that would enrich for ENS progenitors, gut from E11.5 mouse embryos was dissociated into

near single cell suspension and cultured in a medium that supports growth of NCCs. One day later, characteristic colonies appeared that were composed mostly of flat cells with short cytoplasmic processes (Figure 14d). By day 7, these colonies were larger and their cells started to pile up (Figure 14e) and within two weeks formed spherical structures, called neurosphere-like bodies or NLBs, which eventually detached and floated in the medium (Figure 14f).

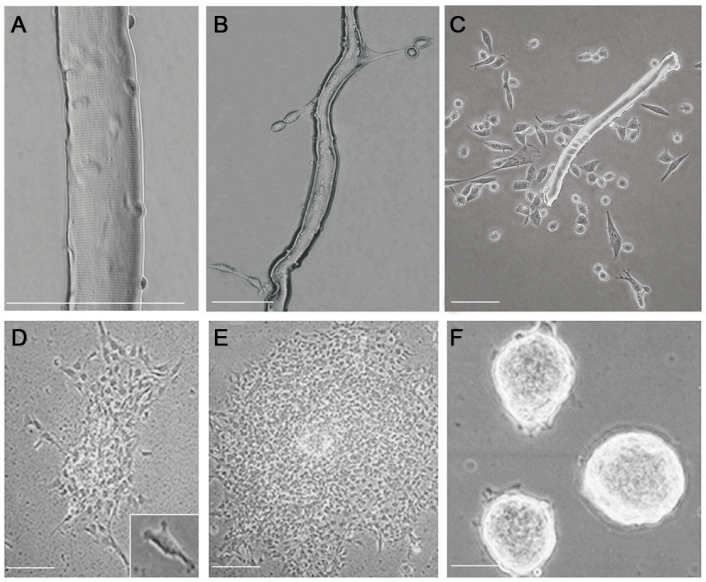

Figure 14: Phase contrast images of MPCs and NCCs (bar: 10 μm).

In order to verify the enhancement of maturation of myogenic cells living in co-culture with neuronal stem cells, we performed an experiment in which MPCs have been cultured at different concentrations with neurospheres. Throughout myogenic conditions for 2 weeks, we cultured them using the following proportions: MPCs-EPCs 1:0, 1:0.5, 1:1, 1:2, and 0:1.

As first step, we determined using western blotting analysis the amount of two specific proteins: (i) β-III tubulin, which is the major component of microtubules, essential cell cytoskeleton proteins involved in mitosis, cytokinesis and transport of vesicles and organelles; and regarded as a neuron-specific marker, and (ii) desmin, an intermediate filament protein of both smooth and skeletal muscles. Cells were detached and proteins were extracted and quantified for all five conditions.

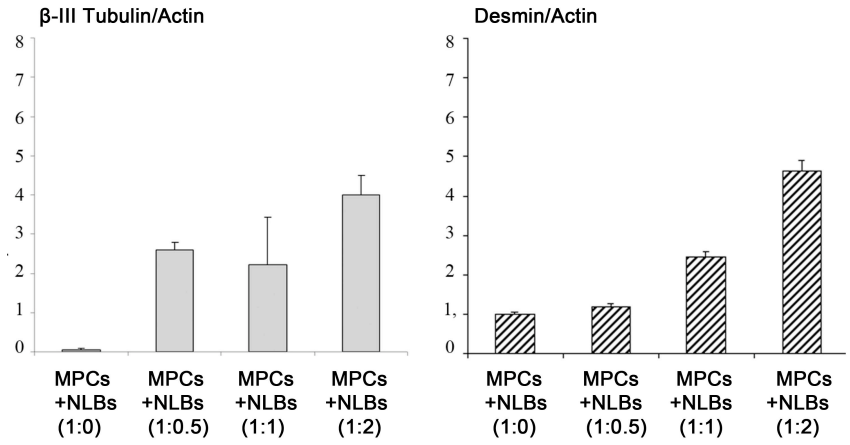

Figure 15: Western blotting analysis of β-III tubulin and desmin. Of all conditions, the highest level of proteins detected was on ratio 1:2.

Figure 15 reports a representative record of western blotting of cells at each ratio. The outcome demonstrates that desmin has an increasing linear trend, and its highest expression was detected with 1:2 ratio of MPCs and NLBs respectively. On the contrary, β-III tubulin pointed up a non-linear tendency due to an higher standard deviation on 1:1 ratio. For this reason, our records did not established which is the best condition among our four concentrations of NLBs.

An indirect evidence of what we discussed above is reported in the following figure. After two weeks in co-culture, MPCs and NLBs gave rise a huge amount of myotubes demonstrating that this protocol enhances myogenic differentiation. However, the enhancement is not only related to the number of myotubes, but also to their sarcomeric bands. In fact, we were able to detect the typical stripes present on skeletal muscles (Figure 16, arrowheads).

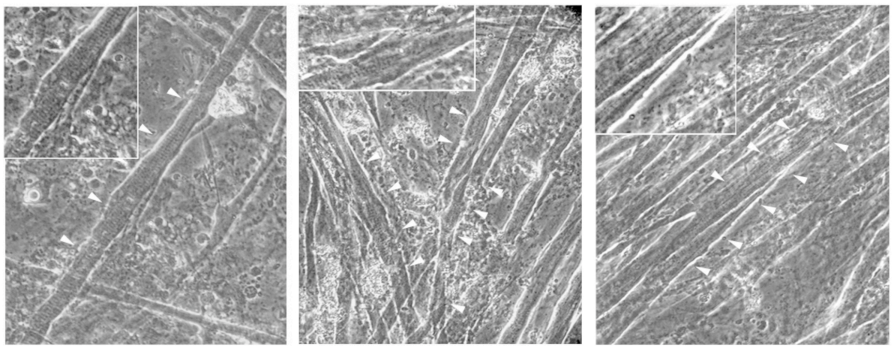

Figure 16: Phase contrast images showed an increased number of myotubes after two weeks of co-culture, giving evidence that the presence of NLBs improves the MPCs differentiation: sarcomeric bands into myotubes (arrowheads).

To examine whether co-cultured cells express troponin I and GFP proteins, immunofluorescence analysis were performed. Our data clearly indicated that in such conditions cells expressed both myogenic and neural markers. Most important, our results indicated that MPCs and NLBs co-localized, as reported in the following figure.

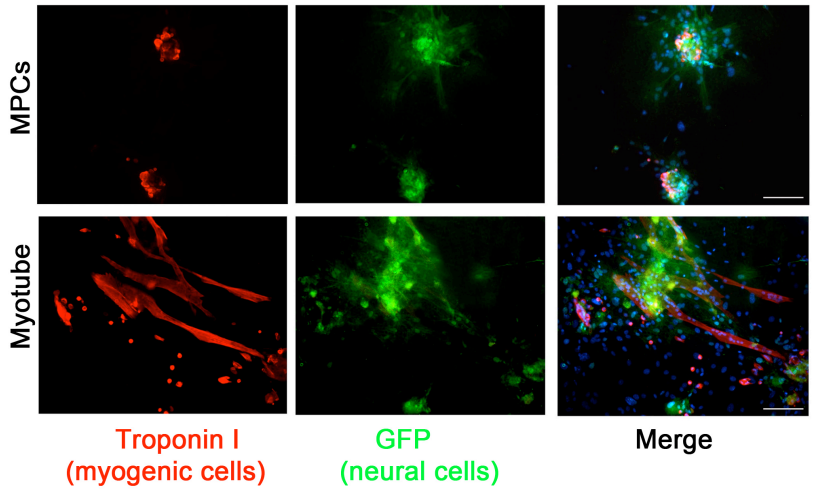

Figure 17: Immunofluorescence analysis for Troponin I and GFP highlighting the co-localization of MPCs and NLBs (bar: 10 µm).

In conclusion, these results underlined that NLBs could improve the differentiation of MPCs promoting the formation of sarcomeric stripes onto myotubes, and increasing the desmin expression of MPCs. As future prospective, we need to further investigate the relationship between MPCs and NLBs, and in particular if the synapses are involved. Secondly, we will need to verify if the seeding on a biocompatible polymer influences the behaviour of neural cells. Lastly, these *in vitro* data must be confirmed with *in vivo* skeletal and smooth muscle differentiations.

Chapter III

3. Introduction

3.1.1 Smooth muscle stem cells in adults

The formation and remodelling of blood vessels after birth has been thought to occur solely via the proliferation and migration of differentiated endothelial and SMCs from blood vessels established during embryogenesis. In spite of this, recent studies of suggest that vascular progenitors are resident within blood circulation and peripheral tissues, and contribute to the formation of new-vascularization during tissue growth and repair. It was previously thought that mural cells (defined as vascular SMCs and pericytes) were recruited via endothelial-derived signals (Lindahl et al., 1997; Hirschi et al., 1998 and 1999) from local mesenchyme in the region of neo-vascularization or recruited along with endothelial cells from pre-existing vessels (Lindahl et al., 1998) to form the surrounding vessel wall as new vessels form from pre-existing structures. However, the cartoon in figure 18 explains the latest findings suggesting that blood circulation, bone marrow and peripheral tissues may contain mural cell progenitors that lead us to describe the origin, distribution and vascular SM potential of adult stem and progenitor cells (Hirschi et al., 2004).

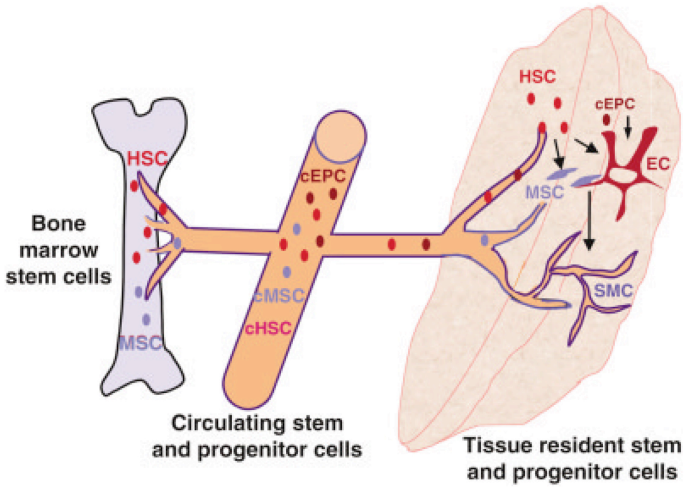

Figure 18: Cells resident within bone marrow, blood circulation, and peripheral tissues can serve as progenitors of mural cells during injury-induced blood vessel formation. HSC, hematopoietic stem cells; MSC, mesenchymal stem cells; cEPC, circulating endothelial precursor cells; cMSC, circulating mesenchymal stem cells; cHSC, circulating hematopoietic stem cells; EC, endothelial cells (from Hirschi et al., 2004).

SMCs possess a structural lattice composed of two primary parts: the cytoskeleton that pervades the cytoplasm and the membrane skeleton that

provides anchorage for the cytoskeleton and contractile apparatus at the cell surface (Table 2).

	Cytoskeleton		Membrane skeleton	
Contractile apparatus	Dense bodies	Cytoskeletal domain	Adherens junctions	Caveolar domain
Actin (SM)	Actin (non-SM)	Actin (non-SM)	Actin (non-SM)	Actin (non-SM) ?
Myosin	α-Actinin	Desmin (or Vimentin)	Filamin	Dystrophin
Tropomyosin	Calponin	Filamin	Calponin	Caveolin
Caldesmon		Calponin	Vinculin	IP_3 receptor
Calponin		Smoothelin	Metavinculin	Na^+/Ca^{2+} exchanger
Myosin light chain kinase		Synamin	Talin	Na^+/K^+ pump
Myosin light chain phosp		Paranemin	Paxillin	
Calmodulin			Tensin	
			α-Actinin	
			Integrins	
			Plectin	

Table 2: Contractile apparatus and cytoskeleton of SMCs (from Small et al., 1998).

The actin filaments of the contractile apparatus are presumed to interface with the cytoskeleton at the cytoplasmic dense bodies and with the longitudinal rib-like arrays of dense plaques of the membrane skeleton that couple to the extracellular matrix. New insights about the role of intermediate filaments in smooth muscle have come from transgenic mice lacking of desmin. Knockout mice reported that desmin protein is dispensable for normal development and viability; however its absence has significant consequences for the mechanical properties of muscle tissue. Thus, the visceral smooth muscles develop only 40% of the normal contractile force and the maximal shortening velocity is reduced by 25-40% (Sjuve et al., 1998). Intermediate filaments therefore play an active role in force transmission and do not contribute solely to cell shape maintenance, as has hitherto been presumed (Small et al., 1998).

3.1.2 Smooth muscle progenitors in peripheral tissues

In addition to progenitors that reside within bone marrow and circulate through blood, Majka and colleagues suggested that smooth muscle and pericytes progenitors reside within peripheral tissues of adults, such as skeletal muscle (Majka et al., 2003). In addition, these are bone marrow-derived progenitors, they expressed SMA and PDGFRβ, and they are also known to regenerate blood cells and vascular endothelial cells. Thus, we can speculate that both vascular endothelial and SMCs progenitors are ultimately derived from the same stem or progenitors that reconstitute all blood cell lineages. This theory is consistent with most of the previously

studies already discussed, which have isolated SMCs progenitors directly from bone marrow or blood circulation while they are in transit to peripheral depots (Hirschi et al., 2004) (Figure 18).

3.2 Smooth muscle differentiation

A promise for regenerative medicine is the differentiation of stem cells into SMCs because it acts as a key role in both vascular and hollow organs tissue engineering.

Cellular differentiation is the process by which cells acquire those cell-specific characteristics that distinguish them from other cell types, and it can be subdivided into the following three major regulatory components:

1. Selective activation of the subset of genes required for the cell's differentiated function;
2. Coordinate control of expression of cell-selective/specific genes at precise times;
3. Continuous regulation of gene expression through effects of local environmental.

The process of SM differentiation and its analysis are extremely complicated due to the plasticity of this cell type and the fact that SMCs originate from multiple precursors throughout the embryo (Majesky MW, 2007).

Previous studies have suggested that various biochemical factors including TGF-β (Transforming Growth Factor β) and the Notch pathway may play important roles in SM differentiation. However, it is not clear yet the downstream signalling components of this transformation and the interactions of these two signalling pathways during the differentiation (Gong et al., 2008; Wang et al., 2004). Nevertheless, the limitations of an analysis *in vitro* of differentiated smooth muscle cells culture should be always taken into consideration because it is not known to which extent differentiation models *in vitro* recapitulate both differentiation and cell maturation *in vivo* (Xie et al., 2011). Even though *in vitro* models are a very powerful to offer insights into the molecular mechanisms, *in vivo* experiments are needed to provide support to the findings from *in vitro* models.

3.3 Amniotic fluid stem cell (AFS)

The amniotic fluid is known to contain a heterogeneous population of cell types derived from the developing foetus (Priest et al., 1978; Polgar et al., 1989). Nevertheless, De Coppi and colleagues described the possibility of deriving pluripotent stem cells from the amniotic fluid: via immunoselection for the antigen c-Kit (CD117), AFS represents about 1% of the whole cells of human amniocentesis. Human AFS are capable of extensive self-renewal and give rise to adipogenic, osteogenic, myogenic, endothelial, neurogenic, hepatogenic lineages were reported (De Coppi et al., 2007), and they also have the potential to differentiate into cardiomyocytes (Bollini et al., 2011). Rodent and murine AFS cells have similar characteristics to human AFS cells. Rodent AFS in terms of *in vitro* proliferation and differentiation properties, while murine AFS cells express markers of embryonic and adult stem cell types (De Coppi et al., 2007). Ditadi and colleagues demonstrated that human and murine AFS are able to generate hematopoietic lineages both *in vitro* and *in vivo* (Ditati et al., 2009).

AFS cells represent a novel class of pluripotent stem cells of foetal origin with intermediate characteristic between embryonic and adult stem cells, the presence of both embryonic and mesenchymal stem cell markers and the capability to differentiate into lineages representative of all embryonic germ layers are their main characteristics. The surface markers that characterized AFS are both mesenchymal and neural cells, but not ES cells. The antigen c-kit is known to be the receptor of stem cell factor and related to gameto and melanogenesis, and homeostasis (Shaw et al., 2011). AFS are positive for CD29, CD44 (hyaluronan receptor), CD73, CD90, and CD105 (endoglin) and they are positive also for stage-specific embryonic antigen (SSEA)-4, also expressed by ES cells. Besides, more than 90% of the cells express the transcription factor Oct4, associated with the maintenance of the undifferentiated state and the pluripotency of ES and EG cells (Pan et al., 2002). AFS can be steadily expanded in cultures, has a typical doubling time of 36 h and do not need any feeder layer. If injected *in vivo*, these cells highlighted no evidence of tumour growth in severe combined immunodeficient mice. They appeared to be less plastic than ES cells, nonetheless reproducibility of the generation and differentiation of these

cells has not yet been widely reported and future studies are required to assess the potential use of this source for clinical applications. In spite of this, in the paediatric field, AFS could play a crucial role for prenatal diagnosed structural defects giving the possibility to obtain homologous and foetal cells for tissue engineering and for postnatal reconstruction (Pozzobon et al., 2009). These cells have been applied into foetal therapy, and our group demonstrated a feasible way to do in-utero autologous AFS transplantation in sheep (Shaw et al., 2011).

Their harbour presents specific advantages in comparison to other stem cell populations:

- They can be easily harvested through amniocentesis (non-invasive approach).
- They do not form tumours after implantation *in vivo* (De Coppi et al., 2007).
- Obtaining them during pregnancy is harmful neither to the mother nor to the foetus (Cananzi et al., 2009).
- Express embryonic and adult stem cell markers.
- Has been done in humans.
- Feeder not required for culturing *in vitro*.
- They maintain the potential up to 250 passages without telomerase length change.
- They did not show teratoma formation after *in vivo* injection (De Coppi et al., 2007).
- Broadly multipotent.

Nevertheless, AFS presents some limitations such as (Hipp et al., 2008):

- Full potential not known.
- Patient-specific.
- Allogenic and autologous transplantation if banked.

In addition, recent papers have demonstrated that, when injected in models of organ damage and development, AFS are able to:

- Engraft into the lung and differentiate into pulmonary lineages (Carraro et al., 2008).
- Integrate into the developing kidney and express early markers of renal differentiation (Perin et al., 2007).

- Repopulate the bone marrow of immunocompromised mice after primary and secondary transplantation (Ditadi et al., 2009).
- Restore the SCs niche in a mouse model of Spinal Muscular Atrophy (data under review).

In our study, we combined the use of viral transduction and growth factors (TFG-β and PDGF-β) to differentiated AFS through SM lineage. Thanks to a lentivirus encoding α-smooth muscle actin under the Zs-Green promoter, we were able to track transduced cells demonstrating that our cells were successfully differentiated *in vitro* into SM lineage under functional and molecular aspects.

Human amniotic fluid stem cells can functionally differentiate along smooth muscle lineage

3.4.1 Background

Replacement or regeneration of functional tissue following loss due to congenital defects is one of the most important challenges of regenerative medicine in Paediatrics. This field has emerged as a potential strategy for the replacement of various tissues, spanning from urogenital (Atala A., 2009), cardiovascular (Ott et al., 2008), upper respiratory tract (Macchiarini et al., 2008; Baiguera et al., 2010), lung (Ott et al., 2010) to liver (Uygun et al., 2010). Tissue engineering entails the use of structurally and functionally defined scaffold provisions that might be either natural or synthetic combined with the seeding of allogeneic or autologous cells of a single or a number of different cell types.

SMCs play a pivotal role in the functionality of numerous tissues and organs, including the vasculature, gastrointestinal tract, urinary bladder, respiratory tract and reproductive tract. Several cellular tissue-engineering approaches have investigated the use of smooth muscle cells in the reconstruction of hollow organs, including the oesophagus, intestine, internal anal sphincter and blood vessels. Regarding the developmental origin and phenotypic characteristics of SMCs, a remarkable heterogeneity has been described (De Coppi et al., 2007). Moreover it has been described that SMCs can shift reversibly along a continuum from a quiescent, contractile phenotype to a synthetic phenotype, which is characterized by proliferation and extracellular matrix (ECM) synthesis (Beamish et al., 2010; Shen et al., 2006).

The use of SMCs or for that question any cell type, as part of a tissue-engineering approach for functional tissue replacement requires a consistent expansion of cells *in vitro*, whilst minimizing the processes of dedifferentiation and/or controlling the processes of cellular differentiation towards the desired cellular phenotype.

The generation of tissue engineered structures for clinical application requires the isolation and expansion of large numbers of cells, maintaining cellular phenotype and physiology without inducing events of cellular senescence and dedifferentiation. The use of stem cells differentiated towards SM phenotype in this frame may have a key role in both vascular and hollow organs tissue engineering, holding a promise for regenerative

medicine applications because they are able to overcome some of the hurdles posed by the limited expansion of differentiated smooth muscle cells.

For our experiments we focused our attention on amniotic fluid stem cells (AFS), representative of about 1% of the whole cells in cultures of human amniocentesis specimens obtained for prenatal genetic diagnosis and immunoselected for c-kit (CD117) marker of differentiation (De Coppi et al., 2007). We now describe the generation of SMCs starting from human AFS cultures using a combined functional analysis approach testing their molecular, electrophysiological and metabolic properties.

3.4.2 Materials and Methods

Human amniotic fluid stem cells isolation

Human amniotic fluid stem cells (hAFSC) were prepared according to methods previously described (De Coppi et al., 2007). Samples of amniotic fluid were collected by amniocentesis from women (gestational age 14-25 weeks) during routine prenatal screening, after a written consent was obtained. Samples were spun at 1500 rpm and pellets re-suspended and seeded in Chang Medium [α-MEM medium (Invitrogen) containing 15% FBS, 1% glutamine and 1% penicillin/streptomycin (Gibco), supplemented with 18% Chang B and 2% Chang C (Irvine Scientific)] at 37°C with 5% CO2 atmosphere. After 3 days, non-adherent cells and debris were discarded and the adherent cells cultivated in pre-confluence. Adherent cells were then immunomagnetically sorted for the expression of the stem marker c-kit using a mouse monoclonal anti-c-kit (CD117) antibody (Santa Cruz, CA) and an anti-mouse IgG CELLection Dynabeads M-450 antibody (Miltenyi Biotech). c-kit$^+$ hAFS cells were reseeded at a density of $2x10^3$ cells/cm^2, cultured in Chang medium in 5% CO_2 at 37°C, expanded and subsequently cloned by limiting dilution and maintained in optimal culture condition of subconfluency (maximum 50%).

Viral transduction

hAFSC were transduced according to methods previously described (Liu et al., 2010). hAFSC at 10^5 cells for each well were transfected using a lentiviral vector in presence of 8 μg/ml polybrene (1x). Virus was then removed 72 hours after infection, cells were monitored under fluorescence microscope, washed twice with PBS and then Chang medium was added.

Differentiation of human amniotic fluid stem cells

In order to induce smooth muscle differentiation, hAFSC were treated with growth factors [5 ng/ml platelet-derived growth factor (PDGF-β) and 2.5 ng/ml transforming growth factor (TGF-β1)] dissolved in culture media [DMEM medium high glucose (Invitrogen) containing 15% FBS, 1% glutamine and 1% penicillin/streptomycin (Gibco)] up to 21 days. Cell media was changed every 48 hours. To determine a growth curve, cells were cultured in 12-well dishes at 1000 cells/well for 7 days. Cells were trypsinized every day and cell number was assessed by Trypan Blue dye and counted in a Burker chamber.

RNA extraction, qPCR and Real Time PCR

Total cellular RNA was isolated from cell cultures using TRIzol. cDNA was synthesized from RNA using SuperScript™ II Reverse-Transcriptase reagents (Invitrogen) according to the manufacturer's instructions. Suitable Real Time PCR oligonucleotide primers were manually designed for each of the genes to assure maximal efficiency and sensitivity. Qualitative PCR was first performed with Taq polymerase protocol according to the manufacturer (Invitrogen). Real-time PCR was then, performed using the default thermocycler program for all genes: 3 minutes of pre-incubation at 94°C followed by 50 cycles for 30 seconds at 94°C, 30 seconds at 60°C and 45 seconds at 72°C. Individual real-time PCR reactions were carried out in 30 μl volumes in a 96-well plate (Applied Biosystems™, London, UK) containing 8 μl DEPC water, 1 μl of sense and antisense primers (10 μM) and 15 μl SYBR Green with ROX ® plus 5 μl of sample. Each experiment was repeated in triplicates, and quantitative PCR analysis was performed in triplicates and analyzed with Delta Ct-method. GADPH was used for

normalization. As positive control a homogenized sample from human foetal intestine was used.

Immunofluorescence

Cover glass seeded with 1000 cells/cm^2 were washed thoroughly with PBS (Phosphate Buffer Saline, GIBCO) and fixed every 7, 11, 17 and 21 days in a solution of PFA 4% (Sigma-Aldrich) for 15-20 minutes. Cell were processed in 0.5% Triton, incubated with 500µl of solution of Bovine Serum Albumin (Sigma-Aldrich) 3% in PBS for 30 minutes to block non-specific binding sites. Primary antibody (Supplementary methods) was incubated for 1 hour at room temperature. Slides were then rinsed quickly with the solution of 3% BSA in PBS and left to incubate with secondary antibody (Supplementary methods) for 1 hour at room temperature. Slides were then mounted with fluorescent mounting medium with DAPI at the concentration of 1.5 µg/ml (Vectashield) on a polylysine slide (ThermoScientific) and observed under epifluorescence microscope (ZEISS Axiophot). To generate a positive control for immunofluorescence, four days old pup rats were sacrificed; 4 cm small intestine segment was tied with re-absorbable woven suture and cut as previously described. The segment was thoroughly rinsed 3-4 times in HBSS and incubated at 37°C for 90 minutes in 0.25% Trypsin-EDTA solution. By mechanical shear the cells were detached with care from the intestine wall and re-suspended in growth medium (DMEM, 15% FBS, 1% penicillin-streptomycin).

Transmission electron microscopy

Cells were re-suspended in 10% BSA (Sigma-Aldrich) and PBS and fixed in 2.5% glutaraldehyde in 0.1M cacodylate buffer (pH 7.2) for 18-24 hours, at room temperature. After the fixation the following steps were performed to prepare the sample for TEM analysis of Osmium Tetroxide, Alcohol and Propylene Oxide/Resin (Supplementary methods). Thin sections (approximative 70 nm) were cut by an ultracut microtome. The sections were collected on TEM copper grids, post-stained with 0.4% lead citrate in 0.4% NaOH for 4 - 10 minutes and rinsed with ultra-pure water. The TEM images of these sections were taken with transmission electron microscope

using a digital camera. The images were further processed (contrast enhancement) using standard imaging software.

Electrophysiology

Dispersed cells were allowed to settle and adhere to the bottom of a 1 ml perfusion chamber mounted on the stage of a Nikon inverted microscope and were perfused with bathing solution at 1-3 ml/min. Electrophysiological studies were performed at room temperature (22-25°C) within 8 hours of dispersion. Whole cell recordings of current employed the nystatin perforated-patch technique using an Axopatch 1D amplifier (Axon Instruments, Foster City, CA). Recording was initiated when the access resistance had stabilized at < 20 MΩ and series resistance compensation up to 80% was often used. Currents were filtered at 500Hz and sampled at 2 kHz. Capacitive currents were compensated online using amplifier circuitry and linear leakage corrected as assessed at negative potentials. Electrophysiological studies were performed with cells bathed in Ringer solution containing (in mM) 130 NaCl, 5 KCl, 1 $CaCl_2$, 1 $MgCl_2$, 20 HEPES, and 10 D-glucose, adjusted to pH 7.4 with NaOH. The recording electrode solution contained (in mM) 30 KCl, 100 potassium aspartate, 10 NaCl, 20 HEPES, 1 $MgCl_2$, 1 EGTA, and 0.4 $CaCl_2$, adjusted to pH 7.2 with NaOH. Electrodes were filled at the tip with filtered solution and then back-filled with solution containing 250 μg/ml nystatin. Krebs bicarbonate solution contained (in mM) 116 NaCl, 5 KCl, 2.2 NaH_2PO_4, 25 $NaHCO_3$, 1.2 $MgSO_4$, 2.5 $CaCl_2$, and 10 D-glucose, equilibrated with 5% CO_2 95% O_2. Drugs (4-aminopyridine, tetraethylammonium, iberiotoxin, carbachol) were prepared from stock solutions in distilled water and diluted into the appropriate bathing solution. In the electrophysiology studies, drugs were applied focally to cells (Picospritzer II; General Valve, Fairfield, NJ) with the concentration reported being that in the application pipette.

Metabolic assay

Two different types of culture media were employed: DMEM which contains 25mM D-glucose, sodium pyruvate, Sodium Bicarbonate

($NaHCO_3$) (44mM) and DMEM with Sodium Bicarbonate ($NaHCO_3$) (44mM) and no glucose, supplemented with 25mM [U-^{13}C] D-glucose.

Both undifferentiated and differentiated cells were cultured in optimal conditions (see above) in hermetic screw caps 25cm^2 flasks (Corning, Sigma-Aldrich) at 1000 cells/cm^2. Media supplemented with [U-^{13}C] D-glucose was substituted to culture media and flasks were sealed for 4 hours. CO_2 production was determined on an isotope ratio-mass spectrometer after CO_2 extraction from culture media by means of acidification with glacial acetic acid. The 13C-to-12C ratios of samples are expressed as differences from the international Pee Dee Belemate limestone (PDB) standard according to the formula $\Delta^{13}C‰ = [(^{13}C/^{12}C \text{ sample} - ^{13}C/^{12}C \text{ standard})/^{13}C/^{12}C \text{ standard}] \times 10^3$. The ratio of $^{13}CO_2$ over $^{12}CO_2$ produced is proportional to the quantity of oxidized glucose.

In vitro contractility assessment

Cell-embedded collagen lattices were employed to measure contractile forces in the smooth muscle differentiated (SMhAFSC) as described previously for other cell source (Tian et al., 2010). In brief, an aliquot containing 6x10^5 cells/ml was mixed with soluble type I collagen (1 mg/ml, BD Biosciences, Franklin Lakes, NJ) containing NaOH, DMEM 10x mixture and $NaHCO_3$ to create a cell-collagen suspension. An aliquot (250 µl) of the cell-collagen suspension was placed onto a 12 well tissue culture plate (BD Bioscience) and allowed to polymerize. A side-by-side comparison of cells with and without collagen mixture was performed that served as negative control. Initial lattice diameter was noted before mechanical release of the cell-collagen lattices for contractile force measurement. The diameter of the cell-collagen lattices was measured after release (from 1 to 10 minutes), and the relative change in diameter calculated. Each experiment was performed in triplicate. Lattices were released after administration of agonist (10 mmol potassium chloride, Sigma) in serum-free medium. The percentage of contraction was calculated by: (Du-Dr)/Du^{x}100 expressed as percentage, where Du and Dr are the diameters of unreleased lattice and released lattice after addition of potassium chloride, respectively.

Proliferation assay

Cell proliferation was quantified by the total cell number as well as the total DNA/well (Cell proliferation kit, Invitrogen). Cells (1.5 x10^3/100 µl) suspended in 10% FCS medium were seeded on 0.1% gelatin-coated flat-bottom 96-multiwell plates and allowed to adhere overnight. Cells were kept in starving conditions (0.1% FBS) for 24 hours, and then media were removed and replaced with 1% FBS medium containing test substances. In order to assess binding effects, the drug was added 1 h prior to the addition of growth factors. After 48 hours, cells were fixed with methanol and stained with Diff-Quik (Fisher). Cell duplication was assessed by counting the total cell number in 10 random fields of each well at X200 with the aid of a 21 mm^2 grid. Moreover, proliferation was assessed by total DNA/ well. After 48 hours, 100 µl of dye binding solution were added to each microplate well and incubated at 37°C for 30 minutes. This incubation period is required for equilibration of dye–DNA binding, resulting in a stable fluorescence endpoint. The fluorescence intensity was read using a fluorescence microplate reader with excitation at 485 nm and emission detection at 530 nm.

Supplementary Methods

Table 3: Primers.

Gene	Sequence	Tm °C	Amplicon (bp)
hDesmin	FW: CCGAGCGGACGTGGATGCAG RV: ATGTCCCTGAGGGCGGCAGT	60 60	198
hMHC 11	FW: GCACGAGATGCCGCCTCACA RV: GGCAAAAGATGGGCCTTGCGTG	60 60	237
hCalponin	FW: TGGCCAGCATGGCGAAGACG RV: CTGTGCCCAGCTTGGGGTCG	60 60	207
hASMA	FW: CCAGTGTGGAGCAGCCCAGC RV: TCACCCCCTGATGTCTGGGACG	60 60	193
hGADPH	FW: AGGCTGGGGCTCATTTGCAGG RV: TGACCTTGGCCAGGGGTGCT	60 60	171

Table 4: Antibodies.

Primary
Mouse monoclonal antibody against human smooth muscle actin hSMA (Dako) [1:100]
Rabbit polyclonal (human, mouse) antibody against smoothelin (Santa Cruz Biotechnology®) [1:100]
Rabbit polyclonal (human, mouse) antibody against desmin (Abcam®) [1:30]
Rabbit polyclonal (human, mouse) antibody against CD31 (Abcam®) [1:30]
Mouse monoclonal (Mouse, Sheep, Human) antibody against pancytokeratine (Abcam®) [1:50]

Secondary
Goat anti mouse IgG 594 nm (Santa Cruz Biotechnology®) [1:150]
Goat anti rabbit IgG 488 nm (Santa Cruz Biotechnology®) [1:150]

Transmission electron microscopy

Negative control cells and differentiated cells were detached with trypsin solution 0.25% and centrifuged for 10 minutes at 4000 rpm. The supernatant was removed and the pellets were re-suspended in 10% BSA (Bovine Serum Albumin (Sigma-Aldrich)) in PBS. The cell suspensions were centrifuged again for 10 minutes at 4000 rpm and the supernatant was removed. The cell pellets were placed in 2.5% glutaraldehyde in 0.1 M cacodylate buffer (pH 7.2) for 18-24 hours, at room temperature in order to fix the cells.

After the fixation the following steps were performed to prepare the sample for TEM analysis:

Reagent	**Time (min)**
Buffer Wash	5
Buffer Wash	5
Osmium Tetroxide	60
Buffer Wash	6
Buffer Wash	6

70% Alcohol	10
Absolute Alcohol	10
Absolute Alcohol	10
Absolute Alcohol	10
Propylene Oxide	10
Propylene Oxide	10
Propylene Oxide/Resin	60
Resin	60
Resin	Overnight

Thin sections (approximative 70 nm) were cut by microtome. Sections were collected on TEM copper grids, post-stained with 0.4% lead citrate in 0.4% NaOH for 4 - 10 minutes and rinsed with ultra-pure water. Images were acquired using a SIS Megaview digital camera, and further processed (contrast enhancement) using standard imaging software.

Viral Transduction

Genomic sequences

Alpha smooth muscle actin promoter (P-αSMA) was amplified with polymerase chain reaction from human genomic DNA using the following primers (table 5).

Table 5: Primers sequences.

P-αSMA	FW: ACAACAATCGATAACAGCTGGTCATGGCTGTA RV: TGTTGTACCGGTGCATGAACCCAGCCAAATCC

The underlined sequences represent the restriction sites ClaI (ATCGAT), AgeI (ACCGGT), or NheI (GCTAGC). The promoter sequences for P-αSMA include 1438 bp upstream and 29 bp downstream of the transcriptional start site. The sequence was legated into a lentiviral vector (Clontech Laboratories Inc., Mountain View, CA) upstream of ZsGreen (P-αSMA) between ClaI and AgeI restriction site for P-αSMA.

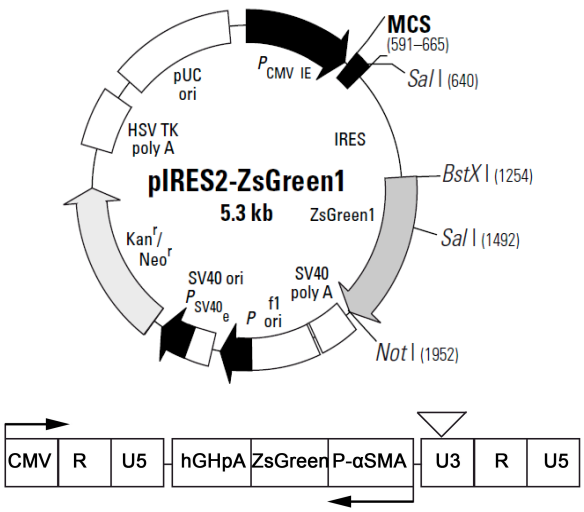

Figure 19: Virus sequence.

pIRES2-ZsGreen1 contains the internal ribosome entry site (IRES) of the encephalomyocaditis virus (ECMV) between an MCS and the *Zoanthus sp.* green fluorescent protein (ZsGreen) coding region. This design permits both the gene of interest (cloned into the MCS) and the ZsGreen1 gene to be translated from a single bicistronic mRNA. pIRES2-ZsGreen1 is designed for the efficient selection (by flow cytometry or other methods) of transiently transfected mammalian cells expressing ZsGreen1 and the protein of interest. This vector can be used to obtain stably transfected cell lines without time-consuming drug and clonal selection. As a result, mammalian cells transfected with this vector will express the green fluorescent protein when transcription of αSMA sequence is activated. Cells expressing ZsGreen (excitation and emission maxima: 496 nm and 506 nm, respectively) can be detected by fluorescence microscopy or flow cytometry (figure 24).

For the transfection HEK293T packaging cell line was used, a specific cell line originally derived from human embryonic kidney cells grown in tissue culture. These cells retain the gag, pol and env genes while the viral genome is replaced by the engineered transgene of choice. These cells were seeded on 10 cm plates and transfected the following day with 15 µg of vector by calcium phosphate DNA precipitation. There were grown as a monolayer in DMEM to confluency and a high titer virus producer clone was identified. The virus was harvested 24 hours post transfection, filtered through 0.45 µm filter (Millipore, Bedford, MA), pelleted by ultracentrifugation (50.000 g at

4°C for 2 hours) and re-suspended in fresh medium, 6 µg/ml of protamine sulphate (Sigma, MO) and 1.23M KCl (Sigma). Titers of lentiviral preparations were determined using 293T/17 cells and ranged between 107-108 IFU/ml.

3.4.3 Results

Amniotic fluid stem cells were cultured for 7 days in both differentiated and undifferentiated state to test their growth capacity (figure 20a). During the first three days, there were no significance difference between hAFSC and SMhAFSC whereas from the 4^{th} day, SMhAFSC delayed their proliferation rate ($p < 0.001$).

Conventional and quantitative PCR were performed to describe the pattern of expression of some markers typically present in smooth muscle differentiation: human Smooth Muscle Actin-α (h-αSMA), human desmin (h-Des), human calponin (h-Calp). At 7^{th}, qPCR revealed that αSMA is highly expressed in SMhAFSC (7d) compared to the control undifferentiated (c). On the other side, only differentiated cells expressed desmin and calponin, markers for smooth muscle (figure 20b).

Moving towards real-time PCR, αSMA transcriptional level 7^{th} day to 21^{st} day, being significantly increased after 11 days of differentiating conditions ($p < 0.01$). Conversely, desmin expression during the differentiation of hAFSC has an oscillatory pattern: high in the earlier stages ($p < 0.01$), decreasing and increasing again in late stage of differentiation (figure 20c). However, desmin expression level after 7 days of differentiated are significantly higher than control ($p < 0.05$). Calponin expression in the differentiated cells has even a higher variability in comparison to αSMA and desmin. Levels of transcription in the first and third time point is significantly higher than the control ($p < 0.01$) although the differentiated cells within the days display an erratic pattern (figure 20c).

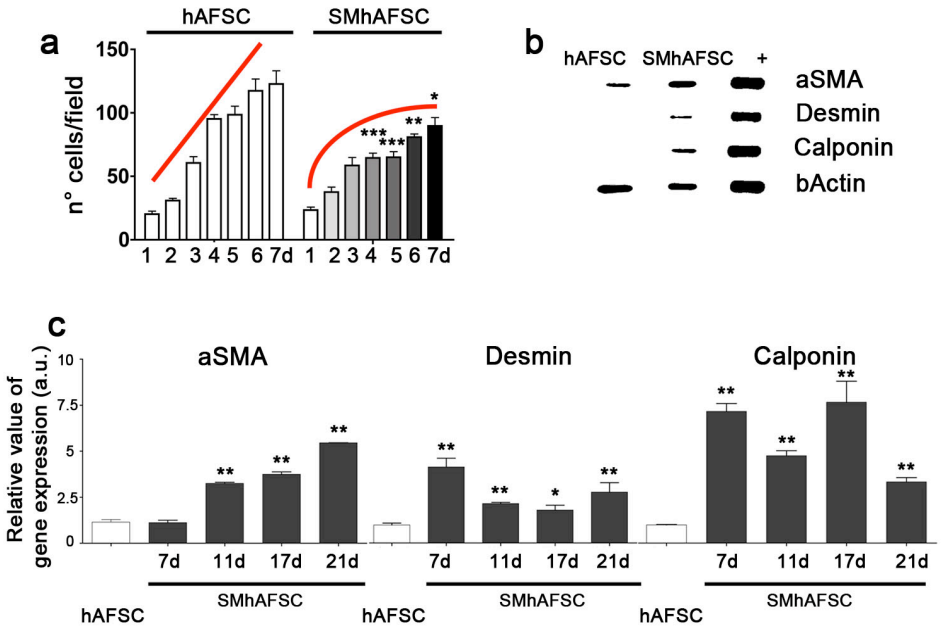

Figure 20: (a) Growth trend of hAFSC and SMhAFSC cultured for 7 days. *, P < 0.05; **, P < 0.01; ***, P < 0.001. (b) Semi-quantitative PCR for αSMA, desmin and calponin in hAFSC, SMhAFSC and SMCs (+). (c) mRNA expression of smooth muscle markers analyzed after 7, 11, 17 and 21 days by Real-Time PCR in hAFSC and SMhAFSC. Results for each condition are from triplicate experiments, and values are expressed in relative units as the mean. *, P < 0.05; ** P < 0.01.

To ensure a better characterization of cellular morphology and ultra-structure of the differentiated cells was change in comparison of undifferentiated cells, a transmission electron microscopy analysis was performed. TEM analysis was carried out on untreated hAFS cells as a negative control and on hAFS treated with differentiation medium contained TGF-β1 and PDGF-β for 21 days. Images of the sample containing control cells show an average dimension of 20-25 μm, a relatively big nucleus without a recognizable nucleolus. This evidence is coherent with a cell with low metabolism; a different ratio of euchromatin/eterochromatin and rough endoplasmic reticulum is barely visible in these cells. The mitochondria in the control cells are few and appear enlarged. Moreover there is not presence of glycogen depots and scarce spots of intermediate filaments (figure 21a-b).

On the other hand, the differentiated cells (figure 21c-d) show a large nucleus and nucleolus. A prominent quantity of heterochromatin is present in the nucleus, indicating that these cells have a very active metabolism. The rough endoplasmic reticulum is largely present around the nucleus. Mitochondria are few and appear stressed. Their internal structures are not

clearly visible because the magnification is too low. Another important characteristic seen all around the cytoplasm is the presence of multiple glycogen depots, typical feature of SMCs (figure 21e-f). It is possible to see many high-density spots of intermediate filament of actin, usually present in large amount in the structure of smooth muscle cells, being a fundamental part of SMCs' cytoskeleton.

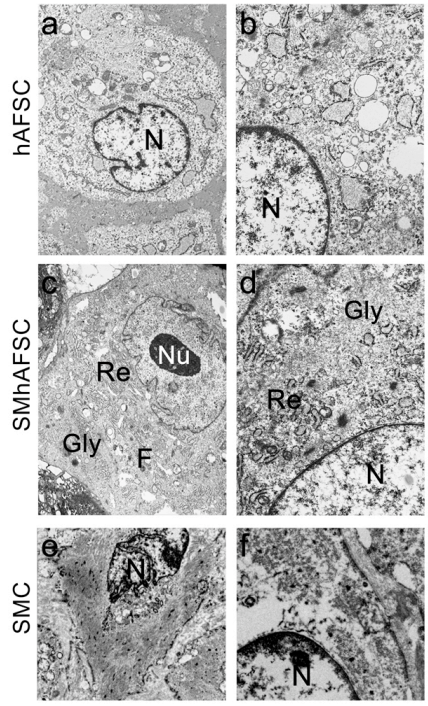

Figure 21: Transmission electron microscopy in (a – b) hAFSC; (c – d) SMhAFSC; (e – f) SMC. Abbreviations: N, nucleus; Nu, nucleolus; Gly, glycogen; F, intermediate filaments; Re, endoplasmic reticulum.

Immunofluorescence staining was performed to follow the progression of differentiation into smooth muscle cells of hAFS cells c-kit$^+$ by the analysis of the principal differentiation marker for smooth muscle lineage like αSMA, desmin and smoothelin. hAFS cells c-kit$^+$ were cultured in differentiation medium rich in growth factor for 21 days and medium was changed every 2 days in all this period.

After 10 days the cultured cells started to express differentiation markers such as αSMA, localized in the intermediate filaments. The differentiated cells (figure 22h) showed a pattern of intermediate filaments of actin similar to the purified positive control cells (figure 22i) that are smooth muscle cells from rat, whereas not treated hAFS cells did not show expression of αSMA (figure 22g). After this treatment with differentiating medium, we were able to demonstrate how hAFS cells express differentiation markers such as αSMA arranged in the structure of cell's cytoskeleton. In the differentiated

culture it is possible to observe several levels of differentiation: there are cells that shown only small intermediate filaments of actin as in an "early" phase of differentiation and there are some cells that have the cytoskeleton of actin completely formed, resembling very similar to the positive control (figure 22p-q).

Desmin is a subunit of the intermediate filaments and therefore is expressed in all the cytoplasm. Differentiated cells (figure 22k) appear positive to desmin as well as the positive control (figure 22l), whereas untreated human AFS cells did not show positivity for this marker (figure 22j). Smoothelin, which is a marker of complete smooth muscle differentiation, appeared present (figure 22n) in differentiated cells, despite being the pattern of expression different from the control (figure 22o) in which smoothelin displayed as cytoplasm rounded granules. The undifferentiated cells did not show positivity to this marker of late differentiation (figure 22m).

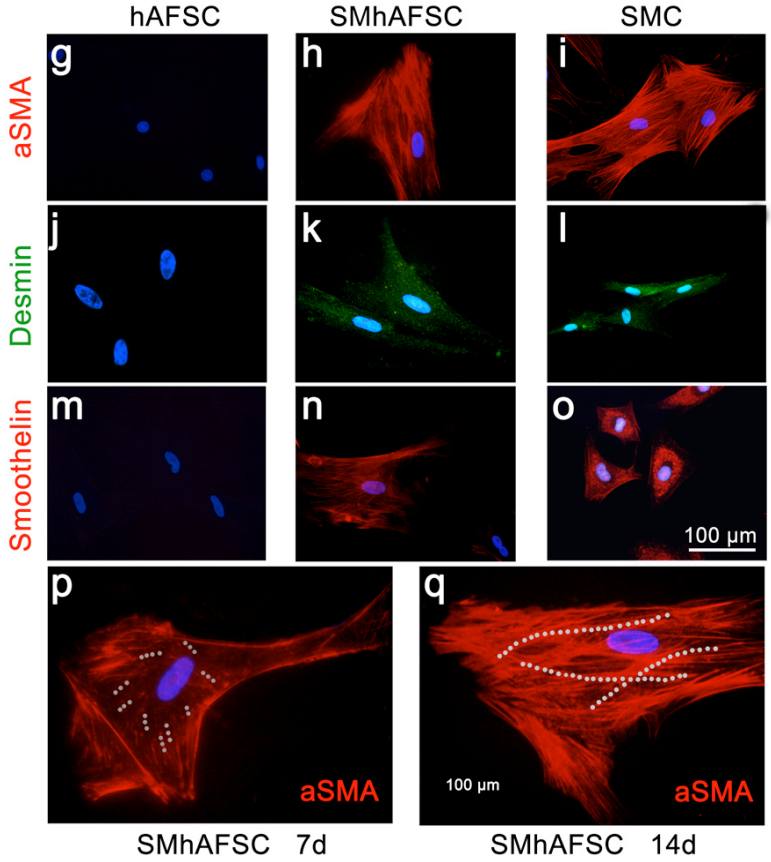

Figure 22: Immunofluorescence analysis for αSMA, desmin and smoothelin. SMhAFSC highlighted positivity in all three smooth muscle markers (h, k, n) compared to smooth muscle cells (SMC) (i, j, o), whilst hAFSC were negative (g, j, m). From 7 to 14 days in differentiation culture, SMhAFSC underlined an increased presence of αSMA microfilaments (p – q).

The lineage commitment through ectodermal and endodermal markers was performed. SMhAFSC highlighted no positivity in both analysis (figure 23b-e) compared to the positive control (figure 23c-f). Undifferentiated cells (figure 23a-d) were negative as SMhAFSC.

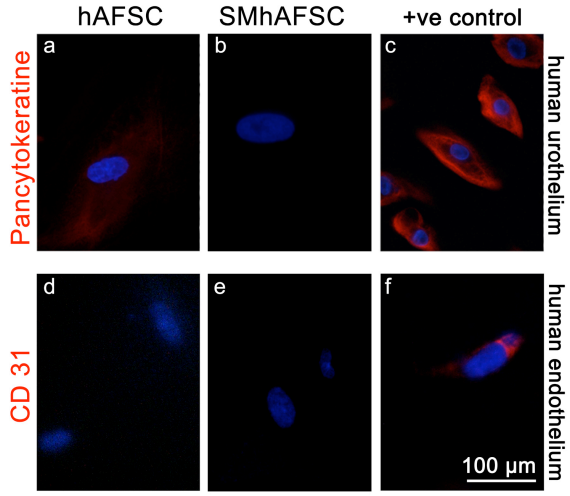

Figure 23: Lineage commitment through human urothelium (upper row) and endothelium (lower row). Immunofluorescence demonstrates negativity in SMhAFSC for both markers underling that our differentiation was done only towards the smooth muscle lineage.

After transduction of human AFS cells with the ZsGreen lentivirus and induced their differentiation, we observed at FACS (Beckton Dickinson) analyses that (figure 24) about 66% of the plotted cells were not committed because didn't express any fluorescent protein and about 33% of the cells expressed ZsGreen fluorescent protein, therefore they had activation of α-SMA promoter and committed to smooth muscle lineage.

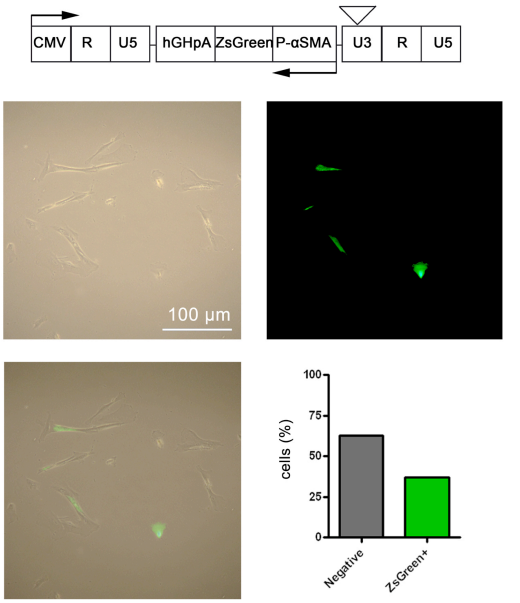

Figure 24: Viral sequence illustrates the presence of αSMA promoter under Zs-Green promoter. Fluorescence images showing transduced hAFSC. The diagram on the right shows the percentage of cells –positive and negative– after transduction.

We used both whole-cell recording and perforated patch to analyze the electrophysiology phenotype of human AFSC and SMhAFSC. The first

method, the whole-cell recording involved recording currents through multiple channels at once, over the membrane of the entire cell. The advantage of this technique is that the larger opening at the tip of the patch clamp electrode provides lower resistance and thus better electrical access to the inside of the cell. Besides that, a disadvantage is that the volume of the electrode is larger than the cell, so the soluble contents of the cell's interior will slowly be replaced by the contents of the electrode. On the other hand, the perforated patch is a variation of whole-cell recording. The electrode solution contains small amounts of an antibiotic that diffuses into the membrane patch forming small perforations in the membrane and providing electrical access to the cell interior. The major advantage is the reduction of the dialysis of the cell that occurs in whole-cell recordings, but the access resistance is higher decreasing the electrical access and the current resolution. Cell depolarization revealed two types of currents: one called K_v, 4-Aminopyridine and iberiotoxin sensitive; and one called K_{Ca}, TEA (TetraEthylAmmonium) sensitive (figure 25a-f).

4-Aminopyridine (dalfampridine) is an organic compound, $H_2NC_5H_4N$ and one of the three isomeric amines of pyridine. Iberiotoxin (a 37-amino acid peptide) is an ion channel toxin purified from the Eastern Indian red scorpion *Buthus tamulus* that selectively inhibits the current through large-conductance calcium-activated potassium channels. Also known as "Potassium channel toxin alpha-KTx 1.3" or IbTx. We reported the current density after incubation with 2 mM TEA (figure 25e-f). SMhASFC showed a slightly decreasing in the K currents (figure 25e) compared to the undifferentiated cells (figure 25f). Iberiotoxin stimulus (200 nM) highlighted a significant decreased in the K currents (figure 25c) while the control cells seem not affected (figure 25d). Whilst giving 5 mM 4-Aminopyridine, only K_v current appeared to be affect in SMhAFSC (figure 25a-b).

A functional analysis was performed to understand if the differentiated cells could produce a contraction like native human smooth muscle cells. Differentiated cells and control cells were tested. They were enclosed in a collagen lattice gel and after the solidification they were immersed in a KCl solution (figure 25k). The following chart (figure 25l) showed that gel itself

did not display any contraction. Untreated hAFS gel demonstrated a very modest contraction, whereas gels containing SMhAFSC showed a strong reduction of gel area. Gel with more differentiated cells (600000/well) had a stronger area reduction, probably because cells had an higher contractile effect on the matrix. These data strongly support that our cells are functionally committed towards smooth muscle lineage.

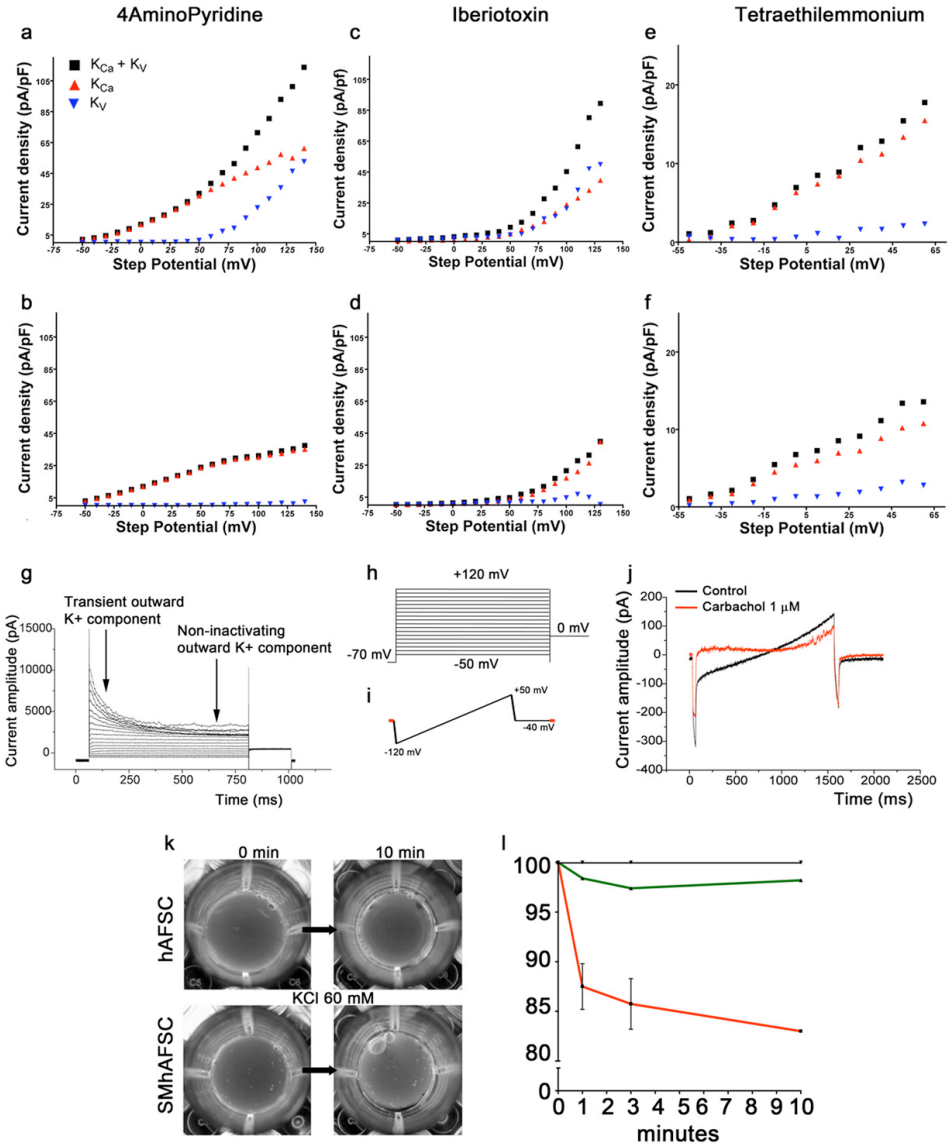

Figure 25: Electrophysiology analysis in SMhAFSC with 4AminoPyridine (a – b), Iberiotoxin (c – d) and TEA (e – f). Schematic representation of the analyzed currents (g – h). Carbachol assay in SMhAFSC (i – j). (k) Collage lattice gel assay in SMhAFSC and hAFSC. Cells were enclosed in a gel and stimulated with KCl 60mM. (l) The chart revealed that gel itself did not display any contraction and hAFS demonstrated a very modest contraction, whilst SMhAFSC showed a strong reduction of gel area.

To determine the level of CO_2 produced by AFS, we used the same protocol that we previously described in chapter one. After 4 hours incubation, we analysed by mass-spectrophotometer the quantity expressed in nmol of CO_2

released in the culture medium. Once again, SMhAFSC showed a higher level of CO_2 compared to hAFSC confirm that the differentiated cells possess a glycolytic metabolism (figure 26a-b).

Proliferation was quantified by total cell number as well as total DNA/well. Cells were starved (0.1% FCS) for 24 hours, media were then removed and replaced with 1% FCS medium containing test substances, like FBS, PDGF-β, FGF-2, TGF-β1. Undifferentiated hAFSC displayed a low response after incubation with growth factors such as PDGF-β, FGF-2, TGF-β1 and PDGF-β/TGF-β1. Conversely, SMhAFSC showed an enhanced proliferative response to growth factor stimulation (figure 26c). In particular, SMhAFSC showed the highest boost on cell proliferation with FBS and PDGF-β/TGF-β1 ($p < 0.001$), with PDGF-β ($p < 0.01$) and a slightly increased with only TGF- β1 ($p < 0.05$).

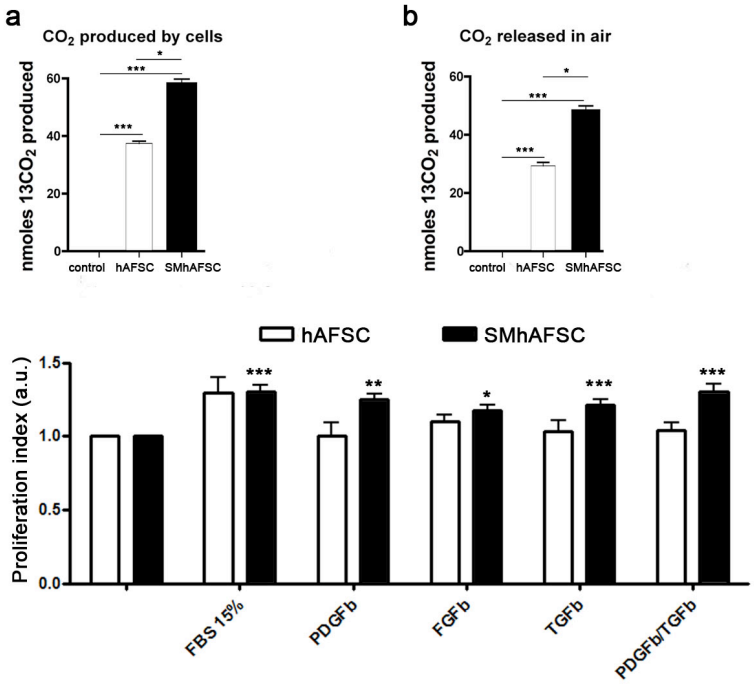

Figure 26: Carbon dioxide measurement in culture medium (a) and in the air (b). SMhAFSC demonstrated to produce an higher amount of CO_2 compared to hAFSC. (c) Proliferation assay in hAFSC (white) and SMhAFSC (black). The highest boosts on cell proliferation were shown with FBS and PDGF-β/TGF-β1 in SMhAFSC compared to hAFSC. *, $P < 0.05$; **, $P < 0.01$; ***, $P < 0.001$.

3.4.4 Discussion

Congenital malformations represent a major cause of disease and death during the childhood and this is mostly due to complex conditions in which either prosthetic materials or transpositions and substitution of different

functional tissue are used because of the lack of tissues able to replace or regenerate damaged organs (Pozzobon et al., 2009).

The generation of tissue engineered structures for clinical application requires the isolation and expansion of large numbers of cells, maintaining their own cellular phenotype and physiology without inducing events of senescence and/or dedifferentiation. Concerning SM applications, a major obstacle that hinders such approach has been finding a reliable and safe source of SMCs that requires a reduced manipulation and can be easily collected. The analysis of mechanisms that direct the process of SM differentiation is extremely complicated by both heterogeneity and plasticity of this cell type and the fact that SMCs originate from multiple precursors throughout the embryo (Majesky MW, 2007). The use of stem cells differentiated towards SM phenotype in this context may provide an alternative treatment for diseases involving hollow organs or sphincters overcoming some of the hurdles posed by the limited expansion of SMCs.

During development, most SM progenitors arise mainly from the splanchnic mesoderm and from the neural crest. At postnatal life, progenitors for SMCs have been found in circulating blood (Hillebrands et al., 2001) and bone marrow (Kashiwakura et al., 2003). It has been already shown that mesenchymal stem cells, which expressed SM proteins, acquired a similar electrophysiological profile to SMCs. *In vitro* differentiation of bone marrow stromal cells induced an enhancement of the calcium-dependent potassium current (IKCa) but, despite specific SM protein expression and modification of electrophysiological properties, differentiated mesenchymal stem cells failed to display contractile properties. These results have underlined the necessity to find the ideal culture conditions to induce a complete developed SMCs functionality. While ES or iPS cells have the limitation of being difficult to program and could lead to tumour formation *in vivo* and adult stem cells are difficult to expand *in vitro*, it would be ideal to have a source of cells capable to overcome all these different problems.

In this study, to generate SMCs we focused our attention on amniotic fluid stem cells, representative of about 1% of the whole cells in cultures of human amniocentesis specimens obtained for prenatal genetic diagnosis and immunoselected for c-kit (CD117) marker of differentiation (De Coppi et

al., 2007). AFS cells can give rise to cell lineages inclusive of the three embryonic germ layers and are positive for a number of surface markers characteristic of mesenchymal and/or neural stem cells. Over 90% of the cells express the transcription factor Oct4, which has been associated with the maintenance of the undifferentiated state and the pluripotency of ES and EG cells. AFS cells appeared to be less plastic than ES cells, nevertheless reproducibility of the generation and differentiation of these SCs has not yet been widely reported and a thorough assessment in regards to SM lineage differentiation has not yet described. The present study demonstrates that a population of adherent cells obtained from amniotic fluid can differentiate into SMCs.

Previous studies of SM differentiation and phenotype modulation indicate that SMCs express the contractile differentiated phenotype when the cells are not in a proliferated state. For this reason, we controlled cell proliferation. TGF-β and PDGF-β has been shown to prevent proliferation, as well as to induce SM markers expression (Kurpinski et al., 2010; Zhang et al., 2009). Moreover, Kurpinski and colleagues described that TGF-β activates Notch signalling to up-regulate SM markers. Particularly, their results highlighted that both TGF-β stimulation and Notch activation were sufficient to induce in the differentiation of human mesenchymal stem cells, and embryonic stem cells (Kurpinski et al., 2010). Although not essential for the acquisition of SM markers, Zhang and colleagues reported that extracellular matrix is able to modulate SMCs (Zhang et al., 2009).

Based on these observations, the effects of media and substrate on the induction of SM phenotype were evaluated. Optimal differentiation occurred when hAFS cells cultured in DMEM high glucose medium supplemented with 15% FBS plus 2.5 ng/ml of TGF-β and 5 ng/ml PDGF-β. At the same time, we additionally exploited a lentiviral transduction using a vector encoding a fluorescent protein linked to the αSMA promoter. Thanks to the acquisition of the marker positivity, we were able to isolate and track those cells that undergo SM differentiation (Liu et al., 2008).

Although, morphologically and physiologically, SMCs form a very heterogeneous population, the majority have some common features such as a spindle shape, low proliferative rate, reduced synthesis of extracellular

matrix, and ligand-induced contractility (Small et al., 1998). It is the sequential expression of cytoskeletal and contractile proteins that generates the diversity of phenotypes ranging from immature cells to mature SMCs expressing the complete repertoire of proteins involved in SM contraction. To establish that certain unique SM markers need to be present, such as αSMA, desmin, calponin, and smoothelin. Although αSMA is an early marker of developing SM, its expression alone does not provide definitive evidence for a smooth muscle lineage. Thus, we chose to evaluate not only αSMA expression, but also the pattern of other smooth muscle markers that are highly restricted to differentiated SM. In particular, smoothelin is not detected in any other cell type and is only expressed in contractile SMCs (van der Loop et al., 1996).

At the genetic level, we found that hAFS cells -like other pluripotent stem cells- express some SM markers at baseline. For this reason, real-time PCR analysis was performed to assess the capacity of our culture conditions to induce an increase in gene expression. hAFS cells acquired typical SMCs morphology and increased in baseline expression of early, mid and late markers of SM differentiation. These findings were confirmed at the protein level in which hAFS showed to be homogeneously positive for αSMA, calponin, desmin and smoothelin but negative for CD31 and pancytokeratine respectively a hallmark of endodermal and ectodermal differentiations.

In literature, it is known that SMCs are highly specialized cells whose principal function is contraction and relaxation. Their ability to contract in response to a physiological stimulus has been considered to be the main proof that myocytes are in a differentiated state. An important focus to this work might be to unravel the potential differentiation towards a vascular or a visceral SMCs phenotype (Chi et al., 2007). In order to better understand this aspect, we performed on our cells an electrophysiological approach. As result, the vast majority of differentiated cells were able to respond to chemical mediators such as carbachol, 4aminopyridine, iberiotoxin and tetraethilammonium with a selective reduction of potassium current as previously described for splanchnic derived SMCs.

In conclusion, we demonstrated that hAFSC, under selective cultural conditions, are able to give rise to functional SMCs. Moreover, transduction process could represents a valuable tool to select SM committed population, and may eventually overcome the well known problem of expanding SM progenitors, making these cells amenable to tissue engineering.

4 References

· Abu-Issa R, Smyth G, Smoak I, Yamamura K, Meyers E. *Fgf8 is required for pharyngeal arch and cardiovascular development in the mouse.* Development, 129:4613-4625, 2002.

· Aguiari P, Leo S, Zavan B, Vindigni V, Rimessi A, Bianchi K, Franzin C, Cortivo R, Rossato M, Vettor R, Abatangelo G, Pozzan T, Pinton P, Rizzuto R. *High glucose induces adipogenic differentiation of muscle-derived stem cells.* Proc Natl Acad Sci., 105: 1226-1231, 2008.

· Amiel J, Sproat-Emison E, Garcia-Barcelo M, Lantieri F, Burzynski G, Borrego S, Pelet A, Arnold S, Miao X, Griseri P, Brooks AS, Antinolo G, de Pontual L, Clement-Ziza M, Munnich A, Kashuk C, West K, Wong KK, Lyonnet S, Chakravarti A, Tam PK, Ceccherini I, Hofstra RM, Fernandez R. Hirschsprung Disease Consortium. *Hirschsprung disease, associated syndromes and genetics: a review.* J Med Genet 45, 1-14, 2008.

· Appell HJ, Forsberg S, Hollmann W. *Satellite cell activation in human skeletal muscle after training: evidence for muscle fiber neoformation.* Int J Sports Med, 9:297-299, 1988.

· Armand O, Boutineau AM, Mauger A, Pautou MP, Kieny M. *Origin of satellite cells in avian skeletal muscles.* Arch Anat Microsc Morphol Exp 72, 163-181, 1983.

· Atala A. *Engineering organs.* Curr Opin Biotechnol 20: 575-592, 2009

· Baiguera S, Jungebluth P, Burns A, Mavilia C, Haag J, De Coppi P, Macchiarini P. *Tissue engineered human tracheas for in vivo implantation*. Biomaterials, 31(34):8931-8, 2010.

· Bajard L, Relaix F, Lagha M, Rocancourt D, Daubas P, Buckingham ME. *A novel genetic hierarchy functions during hypaxial myogenesis: Pax3 directly activates myf5 in muscle progenitor cells in the limb.* Genes & Development, 20(17):2450-64, 2006.

· Barlow AJ, Wallace AS, Thapar N, Burns AJ. *Critical numbers of neural crest cells are required in the pathways from the neural tube to the foregut to ensure complete enteric nervous system formation.* Development 135, 1681-1691, 2008.

· Bedair H. *Matrix metalloproteinase-1 therapy improves muscle healing.* J. Appl. Physiol. 102, 2338-2345, 2007.

· Biressi S, Rando TA. *Heterogeneity in the muscle satellite cell population.* Semin Cell Dev Biol, 21(8):845-54, 2010.

· Bischoff R. *The satellite cell and muscle regeneration.* In: Myogenesis, Mc Graw-Hill, New York. 97-118, 1994.

· Bockman D, Redmond M, Waldo K, Davis H, Kirby M. *Effect of neural crest ablation on development of the heart and arch arteries in the chick*. Am J Anat, 180:332-341, 1987.

· Bollini S, Pozzobon M, Nobles M, Riegler J, Dong X, Piccoli M, Chiavegato A, Price AN, Ghionzoli M, Cheung KK, Cabrelle A, O'Mahoney PR, Cozzi E, Sartore S, Tinker A, Lythgoe MF, De Coppi P. *In vitro and in vivo cardiomyogenic differentiation of amniotic fluid stem cells*. Stem Cell Reviews, 7(2):364-380, 2011.

· Bondurand N, Natarajan D, Barlow A, Thapar N, Pachnis V. *Maintenance of mammalian enteric nervous system progenitors by SOX10 and endothelin 3 signalling.* Development, 133(10), 2075-86, 2006.

· Borello U, Berarducci B, Murphy P, Bajard L, Buffa V, Piccolo S, Buckingham M, Cossu G. *The Wnt/beta-catenin pathway regulates Gli-mediated Myf5 expression during somitogenesis.* Development 133, 3723-3732, 2006.

· Braun T, Rudnicki MA, Arnold HH, Jaenisch R. *Targeted inactivation of the muscle regulatory gene Myf-5 results in abnormal rib development and perinatal death.* Cell, 71(3):369-82, 1992.

· Brunelli S, Relaix F, Baesso S, Buckingham M, Cossu G. *Beta catenin-independent activation of MyoD in presomitic mesoderm requires PKC and depends on Pax3 transcriptional activity.* Dev Biol 304, 604-614, 2007.

· Burns AJ, Delalande JM. N*eural crest cell origin for intrinsic ganglia of the developing chicken lung*. Dev Biol 277, 63-79, 2005.

· Burns AJ, Thapar N, Barlow AJ. *Development of the neural crest-derived intrinsic innervation of the human lung*. Am J Respir Cell Mol Biol 38, 269-275, 2008.

· Cairns J. *Mutation selection and the natural history of cancer*. Nature 255, 197-200, 1975.

· Campanella M, Pinton P, Rizzuto R. *Mitochondrial Ca2+ homeostasis in health and disease*. Biol Res, 37(4):653-60, 2004.

· Campanella M, Casswell E, Chong S, Farah Z, Wieckowski MR, Abramov AY, Tinker A, Duchen MR. *Regulation of the mitochondrial structure and function by the F1F0-ATPase inhibitor protein, IF1*. Cell Metab, 8:13-25, 2008.

· Campanella M, Seraphim A, Abeti R, Casswell E, Echave P, Duchen MR. *IF1, the endogenous regulator of the F1F0-ATP synthase, defines mitochondrial volume fraction in HeLa cells by regulating autophagy.* Biochim Biophys Acta, 1787:393-401, 2009.

· Cananzi M, Atala A, De Coppi P. *Stem cells derived from amniotic fluid: new potentials in regenerative medicine.* Reprod Biomed Online 18(1): 17-27, 2009.

· Carraro G, Perin L, Sedrakyan S, Giuliani S, Tiozzo C, Lee J, Turcatel G, De Langhe SP, Driscoll B, Bellusci S, Minoo P, Atala A, De Filippo RE, Warburton D. *Human amniotic fluid stem cells can integrate and differentiate into epithelial lung lineages*. Stem Cells 26(11): 2902-2911, 2008.

· Chen CN, Li YSJ, Yeh YT, Lee PL, Usami S, Chien S, Chiu JJ. *Synergistic roles of platelet-derived growth factor-BB and interleukin-1beta in phenotypic modulation of human aortic smooth muscle cells.* PNAS 103: 2665-2670, 2006.

· Charge SB, Rudnicki MA. *Cellular and molecular regulation of muscle regeneration.* Physiol Rev, 84:209-238, 2004.

· Chi JT, Rodriguez EH, Wang Z, Nuyten DS, Mukherjee S, van de Rijn M, van de Vijver MJ, Hastie T, Brown PO. *Gene expression programs of human smooth muscle cells: tissue-specific differentiation and prognostic significance in breast cancers.* PLoS Genet 3, 1770-1784, 2007.

· Chinoy MR. *Lung growth and development*. Front Biosci; 8:d392-d415, 2003.

· Christov C, Chretien F, Abou-Khalil R, Bassez G, Vallet G, Authier FJ, Bassaglia Y, Shinin V, Tajbakhsh S, Chazaud B, Gherardi RK. *Muscle satellite cells and endothelial cells: close neighbors and privileged partners.* Mol Biol Cell 18, 1397-1409, 2007.

· Conboy IM, Rando TA. *The regulation of Notch signaling controls satellite cell activation and cell fate determination in postnatal myogenesis.*

Dev Cell, 3(3):397-409, 2002.

· Conboy MJ, Karasov AO, Rando TA. *High incidence of non-random template strand segregation and asymmetric fate determination in dividing stem cells and their progeny*. PLoS Biol. 5, e102. 10.1371/journal.pbio. 0050102, 2007.

· Cornelison DDW, Wold BJ. *Single-Cell analysis of regulatory gene expression in quiescent and activated mouse skeletal muscle satellite cells*. Developmental Biology, 191(2):270-283, 1997.

· Cornelison DD, Wilcox-Adelman SA, Goetinck PF, Rauvala H, Rapraeger AC, Olwin BB. *Essential and separable roles for Syndecan-3 and Syndecan-4 in skeletal muscle development and regeneration.* Genes Dev 18, 2231-2236, 2004.

· Daar AS, Greenwood HL. *A proposed definition of regenerative medicine*. J Tissue Eng Regen Med 1(3): 179-184, 2007.

· De Coppi P, Bartsch G Jr, Siddiqui MM, Xu T, Santos CC, Perin L, Mostoslavsky G, Serre AC, Snyder EY, Yoo JJ, Furth ME, Soker S, Atala A. *Isolation of amniotic stem cell lines with potential for therapy.* Nat Biotechnol 25(1): 100-106, 2007.

· Dey R, Hung K-S. *Development of innervation in the lung*. In: McDonald J, editor. Lung growth and development. New York: Dekker; 244-265, 1997.

· Ditadi A, De Coppi P, Picone O, Gautreau L, Smati R, Six E, Bonhomme D, Ezine S, Frydman R, Cavazzana-Calvo M, André-Schmutz I. *Human and murine amniotic fluid c-kit+lin- cells display hematopoietic activity.* Blood, 113(17):3953-60, 2009.

· Durbec PL, Larsson-Blomberg LB, Schuchardt A, Costantini F, Pachnis V. *Common origin and developmental dependence on c-ret of subsets of enteric and sympathetic neuroblasts.* Development 122, 349-358, 1996.

· Emery E. *The muscular dystrophies.* BMJ. 317; 991-995, 1998.

· Ferrari G, Cusella G, Angelis D, Coletta M, Paolucci E, Stornaiuolo A, Cossu G, Mavilio F. *Muscle regeneration by bone marrow-derived myogenic progenitors.* Science, 279(5356), 1528, 1998.

· Gastaldello A, Callaghan H, Gami P, Campanella M. *Ca2+-dependent autophagy is enhanced by the pharmacological agent PK11195:*

Pharmacological tools in autophagy. Autophagy, 6(5), 2010.

· Gayraud-Morel B, Chretien F, Tajbakhsh S. *Skeletal muscle as a paradigm for regenerative biology and medicine.* Regenerative Med, 4:293-319, 2009.

· Gershon MD, Kirchgessner AL, Wade PR. *Functional anatomy of the enteric nervous system.* In Physiology of the Gastrointestinal Tract, 1, 381-422. New York: Raven Press, 1994.

· Gong Z, Niklason LE. *Small-diameter human vessel wall engineered from bone marrow-derived mesenchymal stem cells (hMSCs).* FASEB J 22, 1635-1648 (2008).

· Gussoni E, Soneoka Y, Strickland CD, Buzney EA, Khan MK, Flint AF, Kunkel LM, Mulligan RC. *Dystrophin expression in the mdx mouse restored by stem cell transplantation.* Nature, 401(6751):390-4, 1999.

· Halayko AJ, Solway J. *Molecular mechanisms of phenotypic plasticity in smooth muscle cells.* J Appl Physiol 90: 358-368, 2001.

· Herrero-Mendez A, Almeida A, Fernández E, Maestre C, Moncada S, Bolaños JP. *The bioenergetic and antioxidant status of neurons is controlled by continuous degradation of a key glycolytic enzyme by APC/C-Cdh1.* Nat Cell Biol, 11(6):747-52, 2009.

· Hill E, Boontheekul T, Mooney DJ. *Regulating activation of transplanted cells controls tissue regeneration.* PNAS 103, 2494-2499, 2006.

· Hillebrands J, Klatter F, van den Hurk B, Popa E, Nieuwenhuis P, Rozing J. *Origin of neointimal endothelium and alpha-actin-positive smooth muscle cells in transplant arteriosclerosis.* J Clin Invest, 107:1411-1422, 2001.

· Hipp J, Atala A. *Sources of stem cells for regenerative medicine.* Stem Cell Reviews, 4(1):3-11, 2008.

· Hirschi K, Rohovsky S, Beck L, Smith S, D'Amore, P. *Endothe-lial cells modulate the proliferation of mural cell precursors via platelet-derived growth factor-BB and heterotypic cell contact.* Circ Res, 84:298-305, 1999.

· Hirschi K, Rohovsky S, D'Amore P. *PDGF, TGF-beta, and heterotypic cell-cell interactions mediate endothelial cell-induced recruitment of 10T1/2 cells and their differentiation to a smooth muscle fate.* J Cell Biol,

141:805-814, 1998.

· Hirschi KK, Majesky MW. *Smooth muscle stem cells.* The Anatomical Record. Part A, Discoveries in Molecular, Cellular, and Evolutionary Biology, *276*(1):22-33, 2004.

· Hollnagel A, Grund C, Franke WW, Arnold HH. *The cell adhesion molecule M-cadherin is not essential for muscle development and regeneration.* Mol Cell Biol 22, 4760-4770, 2002.

· Holterman CE, Le Grand F, Kuang S, Seale P, Rudnicki MA. *Megf10 regulates the progression of the satellite cell myogenic program.* J Cell Biol 179, 911-922, 2007.

· Huang G, Wessels A, Smith B, Linask K, Ewart J, Lo C. *Alteration in connexin 43 gap junction gene dosage impairs conotruncal heart development.* Dev Biol, 198:32-44, 1998.

· Huang S, Wang Z. *Influence of platelet-rich plasma on proliferation and osteogenic differentiation of skeletal muscle satellite cells: an in vitro study*. Oral Surg Oral Med Oral Pathol Oral Radiol Endod, 110(4):453-62, 2010.

· Irintchev A, Zeschnigk M, Starzinski-Powitz A, Wernig A. *Expression pattern of M-cadherin in normal, denervated, and regenerating mouse muscles.* Dev Dyn. 199:326-337, 1994.

· Jain RK. *Normalization of tumor vasculature: an emerging concept in antiangiogenic therapy.* Science 307: 58-62, 2005.

· Jiang X, Rowitch D, Soriano P, McMahon A, Sucov H. *Fate of the mammalian cardiac neural crest.* Development, 127:1607-1616, 2000.

· Jankowski RJ, Deasy BM, Huard J. *Muscle-Derived stem cells*. Gene Therapy, 9(10), 642, 2002.

· Kashiwakura Y, Katoh Y, Tamayose K, Konishi H, Takaya N, Yuhara S, Yamada M, Sugimoto K, Daida H. *Isolation of bone marrow stromal cell-derived smooth muscle cells by a human sm22alpha promoter: In vitro differentiation of putative smooth muscle progenitor cells of bone marrow.* Circulation, 107(16):2078-81, 2003.

· Kassar-Duchossoy L, Giacone E, Gayraud-Morel B, Jory A, Gomes D, Tajbakhsh S. *Pax3/Pax7 mark a novel population of primitive myogenic cells during development.* Genes Dev 19, 1426-1431, 2005.

· Kirby M. *Plasticity and predetermination of mesencephalic and trunk*

neural crest transplanted into the region of the cardiac neural crest. Dev Biol, 134:402-412, 1989.

· Kuang S, Charge SB, Seale P, Huh M, Rudnicki MA. *Distinct roles for pax7 and pax3 in adult regenerative myogenesis.* The Journal of Cell Biology, 172(1):103-13, 2006.

· Kuang S, Kuroda K, Le Grand F, Rudnicki MA. *Asymmetric Self-Renewal and Commitment of Satellite Stem Cells in Muscle. Cell* 129, 5, 999-1010, 2007.

· Kuang S, Rudnicki MA. *The emerging biology of satellite cells and their therapeutic potential.* Trends in Mol. Med. 14, 2, 82-91, 2008a.

· Kuang S, Gillespie MA, Rudnicki MA. *Niche Regulation of Muscle Satellite Cell Self-Renewal and Differentiation.* Cell Stem Cell 2, 22-31, 2008b.

· Kurihara Y, Kurihara H, Oda H, Maemura K, Nagai R, Ishikawa T, Yazaki Y. *Aortic arch malformations and ventricular septal defect in mice deficient in endothelin-1.* J Clin Invest, 96:293-300, 1995.

· Kurpinski K, Lam H, Chu J, Wang A, Kim A, Tsay E, Agrawal S, Schaffer DV, Li S. *Transforming growth factor-beta and notch signaling mediate stem cell differentiation into smooth muscle cells*. Stem Cells, 28(4):734-42, 2010.

· Le Douarin NM, Teillet MA. *The migration of neural crest cells to the wall of the digestive tract in avian embryo.* J. Embryol. Exp. Morphol. 30, 31-48, 1973.

· LeLievre C, Le Douarin N. *Mesenchymal derivatives of the neural crest: analysis of chimeric quail and chick embryos*. J Em-bryol Exp Morphol, 134:125-154, 1975.

· Lindahl P, Johansson B, Leveen P, Betsholtz C. *Pericyte loss and microanerysm formation in PDGF-B-deficient mice.* Science, 277:242-245, 1997.

· Lindahl P, Hellstrom M, Kalen M, Betsholtz C. *Endothelial-perivascular cell signaling in vascular development: lessons from knockout mice.* Curr Opin Lipidol, 9:407-411, 1998.

· Lindsay E, Vitelli F, Su H, Morishima M, Huynh T, Pramparo T, Jurecic V, Orgurinu G, Sutherland H, Scambler P, Bradley A, Baldini A. *Tbx1*

haploinsufficiency in the DiGeorge syndrome region causes aortic arch defects in mice. Nature, 410:97-101, 2001.

· Liu JY, Peng HF, Gopinath S, Tian J, Andreadis ST. *Derivation of functional smooth muscle cells from multipotent human hair follicle mesenchymal stem cells.* Tissue Eng Part A, 16(8):2553-64, 2010.

· Macchiarini P, Jungebluth P, Go T, Asnaghi MA, Rees LE, Cogan TA, Dodson A, Martorell J, Bellini S, Parnigotto PP, Dickinson SC, Hollander AP, Mantero S, Conconi MT, Birchall MA. *Clinical transplantation of a tissue-engineered airway.* Lancet, 372(9655):2023-30, 2008.

· Majesky MW. *Developmental basis of vascular smooth muscle diversity.* Arterioscler Thromb Vasc Biol 27, 1248-1258, 2007.

· Majka S, Jackson K, Kienstra K, Majesky M, Goodell M, Hirschi K. *Distinct progenitor populations in skeletal muscle are bone marrow derived and exhibit different cell fates during vascular regeneration.* J Clin Invest, 111:71-79, 2003.

· Mauro A. *Satellite cell of skeletal muscle fibers*. The Journal of Cell Biology, 9(2):493, 1961.

· McCandless SE, Brunger JW, Cassidy SB. *The burden of genetic disease on inpatient care in a children's hospital*. Am J Hum Genet, 74:121-127, 2005.

· McNamara CJ, Perry TD, Bearce K, Hernandez-Duque G, Mitchell R *Measurement of limestone biodeterioration using the Ca2+ binding fluorochrome Rhod-5N.* J Microbiol Methods, 61:245-250, 2005.

· Menasche P. *Skeletal myoblasts as a therapeutic agent.* Prog. Cardiovasc. Dis. 50, 7-17, 2007.

· Mimeault M, Batra SK. *Recent progress on tissue-resident adult stem cell biology and their therapeutic implications*. Stem Cell Rev 4:27-49, 2008.

· Montarras D, Morgan J, Collins C, Relaix F, Zaffran S, Cumano A, Partridge T, Buckingham M. *Direct isolation of satellite cells for skeletal muscle regeneration.* Science 309, 2064-2067, 2005.

· Morikawa S, Baluk P, Kaidoh T, Haskell A, Jain RK, McDonald DM. *Abnormalities in pericytes on blood vessels and endothelial sprouts in tumors.* Am J Pathol 160: 985-1000, 2002.

· Morrison SJ, Kimble J. *Asymmetric and symmetric stem-cell divisions in development and cancer.* Nature 441, 1068-1074, 2006.

· Nagata Y, Partridge TA, Matsuda R, Zammit PS. *Entry of muscle satellite cells into the cell cycle requires sphingolipid signaling.* J Cell Biol 174, 245-253, 2006.

· Nakamura T, Colbert M, Robbins J. *Neural crest cells retain multipotential characteristics in the developing valves and label the cardiac conduction system.* Circ Res, 98:1547-1554, 2006.

· Niederreither K, Vermot J, Messaddeq N, Schuhbaur B, Chambon P, Dolle P. *Embryonic retinoic acid synthesis is essential for heart morphogenesis in the mouse.* Development, 128:1019-1031, 2001.

· Ott HC, Matthiesen TS, Goh SK, Black LD, Kren SM, Netoff TI, Taylor DA. P*erfusion-decellularized matrix using nature's platform to engineer a bioartificial heart*. Nature Medicine, 14(2): 213-21. 2008.

· Ott HC, Clippinger B, Conrad C, Schuetz C, Pomerantseva I, Ikonomou L, Kotton D, Vacanti JP. *Regeneration and orthotopic transplantation of a bioartificial lung.* Nature Medicine, 16(8):927-33, 2010.

· Owens GK, Wise G. *Regulation of differentiation/maturation in vascular smooth muscle cells by hormones and growth factors*. Agents Actions Suppl 48: 3-24, 1997.

· Owens GK, Kumar MS, Wamhoff BR. *Molecular regulation of vascular smooth muscle cell differentiation in development and disease*. Physiol Rev 84: 767-801, 2004.

· Pan GJ, Chang ZY, Schöler HR, Pei D. *Stem cell pluripotency and transcription factor Oct4.* Cell Res. 12:321-9, 2002.

· Péault B, Rudnicki MA, Torrente Y, Cossu G, Tremblay JP, Partridge TA, Gussoni E, Kunkel LM, Huard J. *Stem and Progenitor Cells in Skeletal Muscle Development, Maintenance, and Therapy.* Mol. Ther. 15, 5, 867-877, 2007.

· Pelicano H, Carney D, Huang P. *ROS stress in cancer cells and therapeutic applications.* Drug Resist Updat, 7: 97-110, 2008.

· Perin L, Giuliani S, Jin D, Sedrakyan S, Carraro G, Habibian R, Warburton D, Atala A, De Filippo RE. *Renal differentiation of amniotic fluid stem cells.* Cell Prolif 40(6): 936–948, 2007.

· Polgar K, Adány R, Abel G, Kappelmayer J, Muszbek L, Papp Z *Characterization of rapidly adhering amniotic fluid cells by combined immunofluorescence and phagocytosis assays.* Am. J. Hum. Genet. 45, 786-792, 1989.

· Priest RE, Marimuthu KM, Priest JH. *Origin of cells in human amniotic fluid cultures: ultrastructural features.* Lab. Invest. 39, 106-109, 1978.

· Punch VG, Jones AE, Rudnicki MA. *Transcriptional networks that regulate muscle stem cell function*. Wiley Interdisciplinary Reviews. Systems Biology and Medicine, 1(1):128-40, 2009.

· Relaix F, Rocancourt D, Mansouri A, Buckingham M. *A Pax3/Pax7-dependent population of skeletal muscle progenitor cells.* Nature 435, 948-953, 2005.

· Rosenblatt JD, Yong D, Parry DJ. *Satellite cell activity is required for hypertrophy of overloaded adult rat muscle.* Muscle Nerve. 17; 608-613, 1994.

· Rossi CA, Pozzobon M, Ditadi A, Archacka K, Gastaldello A, Sanna M, Franzin C, Malerba A, Milan G, Cananzi M, Schiaffino S, Campanella M, Vettor R, De Coppi P. *Clonal characterization of rat muscle satellite cells: Proliferation, metabolism and differentiation define an intrinsic heterogeneity*. Plos One, 5(1), e8523, 2010.

· Rossi CA, Flaibani M, Blaauw B, Pozzobon M, Figallo E, Reggiani C, Vitiello L, Elvassore N, De Coppi P. *In vivo tissue engineering of functional skeletal muscle by freshly isolated satellite cells embedded in a photopolymerizable hydrogel.* FASEB, 25(7):2296-304, 2011.

· Rudnicki MA, Braun T, Hinuma S, Jaenisch R. *Inactivation of myod in mice leads to up-regulation of the myogenic HLH gene myf-5 and results in apparently normal muscle development.* Cell, 71(3):383-390, 1992.

· Rudnicki MA, Le Grand F, MCKinnell I, Kuang S. *The Molecular Regulation of Muscle Stem Cell Function.* Cold Spring Harb Symp Quant Biol 73, 323-331, 2008.

· Sambasivan R, Tajbakhsh S. *Skeletal muscle stem cell birth and properties.* Seminars in Cell & Developmental Biology 18, 870-882, 2007.

· Sasai Y, De Robertis E. *Ectodermal patterning in vertebrate embryos*. Dev Biol, 182:5-20, 1997.

· Schittny JC, Miserocchi G, Sparrow MP. *Spontaneous peristaltic airway contractions propel lung liquid through the bronchial tree of intact and fetal lung explants.* Am J Respir Cell Mol Biol; 23:11-18, 2000.

· Schuchardt A, D'Agati V, Larsson-Blomberg L, Costantini F, Pachnis V. *Defects in the kidney and enteric nervous system of mice lacking the tyrosine kinase receptor Ret.* Nature 367, 380-383, 1994.

· Schultz E. *Satellite cell in normal, regenerating and dystrophic muscle*. Adv Exp Med Biol, 182:73-84, 1985.

· Seale P, Sabourin LA, Girgis-Gabardo A, Mansouri A, Gruss P, Rudnicki MA. *Pax7 is required for the specification of myogenic satellite cells.* Cell 102, 777-786, 2000.

· Seale P, Ishibashi J, Holterman C, Rudnicki MA. *Muscle satellite cell-specific genes identified by genetic profiling of MyoD-deficient myogenic cell.* Dev. Biol. 275, 287-300, 2004.

· Shaw SW, Bollini S, Nader KA, Gastadello A, Mehta V, Filppi E, Cananzi M, Gaspar HB, Qasim W, De Coppi P, David AL. *Autologous transplantation of amniotic fluid-derived mesenchymal stem cells into sheep fetuses.* Cell Transplantation, 20(7):1015-31, 2011.

· Shi X, Garry DJ. *Muscle stem cells in development, regeneration, and disease*. Genes Dev, 20:1692-708, 2006.

· Shinin V, Gayraud-Morel B, Gomes D, Tajbakhsh S. *Asymmet-ric division and cosegregation of template DNA strands in adult muscle satellite cells.* Nat. Cell Biol. 8, 677-687, 2006.

· Sjuve R, Arner A, Li Z, Mies B, Paulin D, Schmittner M, Small JV. *Mechanical alterations in smooth muscle from mice lacking desmin.* J Muscle Res Cell Motil, 19(4):415-29, 1998.

· Small JV, Gimona M. *The cytoskeleton of the vertebrate smooth muscle cell.* Acta Physiol. Scand, 164:341-348, 1998.

· Sparrow MP, Weichselbaum M, McCray PB. *Development of the innervation and airway smooth muscle in human fetal lung.* Am J Respir Cell Mol Biol; 20:550-560, 1999.

· Szabadkai G, Duchen MR. *Mitochondria: The hub of cellular Ca2+ signalling.* Physiology (Bethesda, Md.), 23:84-94, 2008.

· Tajbakhsh S. *Skeletal muscle stem cells in developmental versus*

regenerative myogenesis. Journal of Internal Medicine, 266(4):372-89, 2009.

· Tallquist M, Soriano P. *Cell autonomous requirement for PDGFR_ in population of cranial and cardiac neural crest cells*. Development, 130:507-518, 2003.

· Tedesco FS, Dellavalle A, Diaz-Manera J, Messina G, Cossu G. *Repairing skeletal muscle: Regenerative potential of skeletal muscle stem cells.* The Journal of Clinical Investigation, 120(1):11-9, 2010.

· Tian H, Bharadwaj S, Liu Y, Ma PX, Atala A, Zhang Y. *Differentiation of human bone marrow mesenchymal stem cells into bladder cells: potential for urological tissue engineering.* Tissue Eng Part A; 16(5):1769-79, 2010.

· Tollet J, Everett AW, Sparrow MP. *Spatial and temporal distribution of nerves, ganglia, and smooth muscle during the early pseudoglandular stage of fetal mouse lung development.* Dev Dyn; 221:48-60, 2001.

· Uygun BE, Soto-Gutierrez A, Yagi H, Izamis ML, Guzzardi MA, Shulman C, Milwid J, Kobayashi N, Tilles A, Berthiaume F, Hertl M, Nahmias Y, Yarmush ML, Uygun K. *Organ reengineering through development of a transpantable recellularized liver graft using decellularized liver matrix.* Nature Medicine, 16(7):814-20 2010.

· van der Loop FT, Schaart G, Timmer ED, Ramaekers FC, van Eys GJ. *Smoothelin, a novel cytoskeletal protein specific for smooth muscle cells.* J. Cell Biol, 134:401-411, 1996.

· Vitelli F, Morishima M, Taddei I, Lindsay E, Baldini A. *Tbx1 mutation causes multiple cardiovascular defects and disrupts neu-ral crest and cranial nerve migratory pathways*. Hum Mol Genet 11:915-922, 2002a.

· Vitelli F, Taddei I, Morishima M, Meyers E, Lindsay E, Baldini A. *A genetic link between Tbx1 and fibroblast growth factor signaling.* Development 129:4605-4611, 2002b.

· Wang D, Chang PS, Wang Z, Sutherland L, Richardson JA, Krieg PA, Olson EN. *Activation of cardiac gene expression by myocardin, a transcriptional cofactor for serum response factor.* Cell 105: 851-862, 2001.

· Wang D, Park JS, Chu JS, Krakowski A, Luo K, Chen DJ, Li S. *Proteomic profiling of bone marrow mesenchymal stem cells upon*

transforming growth factor beta1 stimulation. J Biol Chem 279, 43725-43734, 2004.

· Weichselbaum M, Sparrow MP. *A confocal microscopic study of the formation of ganglia in the airways of fetal pig lung.* Am J Respir Cell Mol Biol; 21:607-620, 1999.

· Xie C, Ritchie RP, Huang H, Zhang J, Chen YE. *Smooth muscle cell differentiation in vitro: models and underlying molecular mechanisms*. Arterioscler Thromb Vasc Biol 31, 1485-1494, 2011.

· Yalcin A, Clem BF, Simmons A, Lane A, Nelson K, Clem AL, Brock E, Siow D, Wattenberg B, Telang S, Chesney J. *Nuclear targeting of 6-phosphofructo-2-kinase (PFKFB3) increases proliferation via cyclin-dependent kinases.* J Biol Chem, 284(36):24223-32, 2009.

· Yamagishi H, Maeda J, Hu T, McAnally J, Conway S, Kume T, Meyers E, Yamagishi C, Srivastava D. *Tbx1 is regulated by tissue-specific forkhead proteins through a common Sonic hedge-hog-responsive enhancer.* Genes Dev, 17:269-281, 2003.

· Yanagisawa H, Hammer R, Richardson J, Williams S, Clouthier D, Yanagisawa M. *Role of endothelin-1/endothelin-A receptor-mediated signaling pathway in the aortic arch patterning in mice*. J Clin Invest, 102:22-33, 1998.

· Yntema CL, Hammond WS. *The origin of intrinsic ganglia of trunk viscera from vagal neural crest in the chick embryo.* J. Comp. Neurol. 101, 515-542, 1954.

· Zhang Y, He Y, Bharadwaj S, Hammam N, Carnagey K, Myers R, Atala A, Van Dyke M. *Tissue-specific extracellular matrix coatings for the promotion of cell proliferation and maintenance of cell phenotype.* Biomaterials 30, 4021-4028, 2009.

• Zhou Y, Atkins JB, Rompani SB, Bancescu DL, Petersen PH, Tang H, Zou K, Stewart SB, Zhong W. *The mammalian Golgi regulates numb signalling in asymmetric cell division by releasing ACBD3 during mitosis*. Cell 129, 163-178, 2007.